MEMORANDUM

Subject	Dynamic amplification effects for B-stations due to building response
Project	Verification of the quality and correctness of KNMI seismic recordings Groningen field
Client	Staatstoezicht op de Mijnen (SODM)
Project code	113982
Status	Final
Date	12 June 2019
Reference	113982/19-009.783
Author(s)	ir.
Checked by	ir.
Approved by	ir.
Initials	
Appendices	-
To	SODM dr.
Copy	-

1 INTRODUCTION

1.1 Background

Staatstoezicht op de Mijnen (SODM) requested Witteveen+Bos and TU Delft to perform additional verifications to check the quality of KNMI earthquake recordings for events of the Groningen field.

The first part of the scope of the present study comprises a quality review of all the KNMI records in Groningen over the period January 2014 to December 2018, having magnitude M_L > 2.0. This part of the project has resulted in ref. [3].

The second part, which is reported in this document, comprises a case study based analysis towards the understanding of the system resonance effects that are observed for B-stations (ref. [1]). It has been observed that the vertical motion component in B-stations might be amplified compared to nearby G-station recordings. This observation triggered the study prescribed in this report. The objective is to examine the influence of the building response on the recorded motions and possibly to evaluate the need of a potential more elaborate follow-up study that will go in depth into the topic.

1.2 Scope and limitations

This document reports the investigation on the potential influence of the soil-structure interaction (SSI), and the structure response itself, for B-stations and G-stations. Especially for B-stations concerns have been raised that the signals may be influenced by the fact that these stations are installed in buildings. Here the main concern lies in the fact that the sensors which are located in buildings do not reproduce the actual ground motion characteristics but the response of the building itself. In this study, we try to investigate whether the response of the building affects the recorded signals in the relevant frequency range of interest.[1]

For the purpose of this study, the building (excluding the foundation block) is described with a reduced-order model having an effective lateral stiffness representing the actual stiffness of the building in each direction at its fundamental mode of vibration. The reduced-order model of the building is then attached to a rigid foundation block which is supported by the underlying soil. The foundation block is representative of the actual one, also in terms of the dimensions, in which the sensor is attached at the appropriate location. The dynamic analysis reported in this document includes full consideration of the dynamic soil-structure interaction (SSI). This modelling approach suffices to provide answers to the key questions regarding possible resonance effects of the ground motions caused by the fact that the sensors are attached to the building foundation; a more detailed model of the building is beyond the scope of the present study.

The scope of the quick scan presented in this document comprises:
1 Selection of case studies, identification of station setting and estimation of equivalent system characteristics.
2 Signal processing.
3 Calculation of dynamic frequency response functions (FRFs) based on numerical modelling (with the reduced-order model of the physical system under consideration).
4 Analysis on the observed records and the simulation results.
5 Conclusions and recommendations for further study.

2 SELECTION OF CASE STUDIES AND SET UP OF NUMERICAL MODELS

2.1 Stations selection

Table 2.1 presents the B-stations located in the Groningen field coupled to the closest G-station. In the table, some key features of the couples of stations are listed as well.

Four cases of B-station and G-station couples are chosen for further analysis based on the following:
- An adequate number of reliable signals have been recorded by both B- and G-station of each B-G-couples. In other words, recordings that contain high levels of noise, give the impression that another source has been recorded, or seem to be defected are excluded from the signal selection.
- The building in which the B-stations are located does not have pile foundations.[2]
- The distance between the B- and the G-stations is as small as possible.

[1] Here it should become clear that a sensor positioned in a building measures, in fact, the response of the building itself. However, if the response of the building is such that no resonances of the building-foundation superstructure are found within the relevant frequency range of interest we can safely conclude that the recording itself resembles closely the actual motion of the ground. In contrast, if resonances of the building-foundation superstructure are located within the frequency range of interest then we can conclude that the presence of the building has an influence in the recorded signal and, in fact, what is recorded cannot be genuinely considered as the true 'ground motion'.

[2] Here we clarify that buildings were selected in which no piled foundations are expected based on the layout and the soil properties.

- There is a clear trend in the Fourier Amplitude Spectra (FAS) ratios between B- and G-stations indicating possible influence of the presence of the building and/or SSI. (In order to understand the effect cases with a clear trend are more interesting, rather than the averaged typical effect observed for all B-stations).
- The availability and uncertainty related to the building characteristics. This comprises two elements:
  - Inclusion in ref [2] of a building typology similar to that of the building (B-station) so that the first mode of vibration and the effective properties of the reduced-order model are retrieved.
  - The structural layout of the superstructure building is such that the effective properties of the reduced-order model could be estimated without extensive numerical modelling since the latter falls outside the scope of the present study.

Based on the aforementioned criteria the following four couples of B- and G-stations are selected for further analysis:

- Case 1: BOWW - G190.
- Case 2: BAPP - G670.
- Case 3: BSTD - G220.
- Case 4: BFB2 - G450.

BOWW and BAPP are relatively small/light weight structures, being a wooden shed and garage respectively. BSTD and BFB2 are larger structures, classifying as barns. Selecting two subsets of similar typology serves to be able to observe trends in response function more clearly. Any kinematic interaction effects [1], which are not the focus of the present study that focusses on building resonance, as suggested in [1] should be much more significant for the latter two selected cases since these buildings are much larger and heavier.

Table 2.1 Collection of B-stations with the corresponding closest G-station, including some characteristics of the building in which the B-station is located

Station ID	Location	Closest G-station	Distance between B- and G-station	Brief description	Equivalent typology from ref [2]	Soil profile and expected foundation type
BAPP	Appingedam	G67	1,100 m	garage / shed, 8.5 x 5 m		5 m soft soil, below a few sand layers and then pot clay. Garage probably piled
BFB2	Kolham	G45	1,350 m	barn, 33 x 17 m	De Haver (no house)	sand, interlayered with thin clay layers, Barn probably not piled
BGAR	Garsthuizen	G61	2,600 m	masonry garage, 4 x 3.5 m N-S		12 m of soft soils with at 5 m a loose sand layer. From 13 m and deeper sand. Garage probably piled
BHAR	Harkstede	G39	1,100 m	aluminium / steel barn, 20 x 10 m NW-NE		7 m mix of loose to medium dense sand and clays. Then 5 m sand then few m clay then 4 m sand then clay. Probably not piled
BHKS	Garrelsweer	G29	1,200 m	masonry barn, 20 x 15 m NW-SE		4 m very soft soil, then 1 m sand then 12 m soft soils then sand. Due to barn and age probably not piled
BLOP	Loppersum	G18	1,700 m	concrete/masonry garage, 9 x 3.5 m W-E		10 m soft soil, then sand, based on construction drawing probably not piled

[1] Non-synchronous base excitation' caused by the different arrival times of the waves at different locations below the foundation.

Station ID	Location	Closest G-station	Distance between B- and G-station	Brief description	Equivalent typology from ref [2]	Soil profile and expected foundation type
BMD2	Middelstum	G13	1,500 m	large house with barn, 35 x 25 m, N-S	De Haver	11 m soft soil, then 3 m sand, then pot clay. Massive building probably piled
BOWW	Oosterwijtwerd	G19	420 m	timber shed, 6 x 5 m, W-E		9 m soft soil, 7 m sand/silt/clay, then pot clay. Probably not piled
BSTD	Stedum	G22	1,000 m	masonry barn, 25 x 40 m NE-SW	De Haver (no house)	8 m soft soil, 1 m dense sand, then pot clay. Probably not piled, but we cannot be sure
BUHZ	Uithuizen	G04	860 m	town hall, 40 x 50 m, W-E	Koerierster-weg 20-21	16 m mix of sand and clay, then dense sand. Piled
BWIN	Winneweer	G23	1,360 m	masonry house with basement, 7.5 x 13 m, N-S	Julianalaan 52	7 m soft soil, then 4 m sand, then pot clay. Foundation type unknown
BWIR	Wirdum	G23	1,900 m	shed, 12 x 6.5 m, W-E		7 m soft soil, then 5 m sandy clay and clay, then pot clay. Probably not piled
BWSE	Westeremden	G18	1,700 m	masonry shed (based on QGIS location), 15 x 9 m, NW-SE		8 m mix of sandy clay and clay, then 2 m sand, then 3 m clay, then 3 m sand, then 2 m clay, then 2 m sand, then 3 m clay, then pot clay. Probably not piled
BZN1	't Zandt	G14	840 m	masonry garage, 5.5 x 10,5 m, W-E		11 m clay and sandy clay with lences of sand. Then sand. Important large building, probably piled
BZN2	Zeerijp	G14	1,100 m	masonry house with large barn, 21 x 43 m, W-E	De Haver	4 m soft soil, then 4 m sandy clay and sand, then 3 m soft clay, then sand. Barn probably not piled.

2.2 B-station building equivalent system characteristics

For the setup of the numerical models, the buildings in which the B-stations are located are idealized by discrete systems with a few degrees of freedom which try to mimic the behaviour of the structure in its fundamental mode of vibration. The reduced-order model consists of a massless beam with an assigned bending stiffness EI (where E is the Young's modulus and I the moment of inertia of the equivalent beam), a height (h) and a lumped mass (M) at the top as shown in Figure 2.1. The walls, the columns and, when present, the bracings of the buildings are used for the calculation of the mass (it is assumed that half of this mass is transferred at the position of the lumped mass and half to the base slab) and the bending stiffness EI of the equivalent beam which represents the overall lateral stiffness of the actual building in its fundamental mode of vibration in the different directions. The lumped mass (M) at the top usually corresponds to the mass of the roof of the building. The height (h) of the beam, is approximated by the gutter height.

The idealized system representing the building is clamped on a foundation slab at its centre. The dimensions and the mass of the foundation slab of each building are estimated based on the available data as well. The building-foundation system rests on top of a layered soil medium which extends to infinity in all directions. This way, the building-foundation system is essentially reduced to a few degrees of freedom, however, the

coupled soil-foundation-building system has infinite degrees of freedom due to the presence of the layered soil continuum. The resulting model of the superstructure is illustrated by Figure 2.1.

Figure 2.1 Sketch of the equivalent SDOF-system including the base-slab and the position of the B-station on the slab

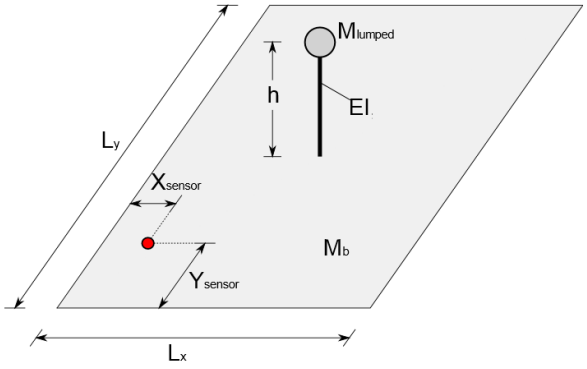

The characteristics of the superstructure equivalent SDOF-system are derived as reported in Appendix I and are summarized in Table 2.2.

Table 2.2 Characteristics of the equivalent systems that represent the buildings in which B-stations are located

Station	Slab dimensions	Slab mass	Lumped mass	Flexural rigidity		Effective height	SDOF eigenfrequency	
	L_x x L_y	M_b	M_{lumped}	EI_x	EI_y	h	f_x	f_y
	[m x m]	[kg]	[kg]	[MNm^2]	[MNm^2]	[m]	[Hz]	[Hz]
BOWW	6 x 6	9,500	4,500	22	22	2.40	10.37	10.37
BAPP	5 x 8.5	12,200	4,300	0.69	0.795	2.40	1.88	2.02
BSTD	25 x 40	250,000	432,000	1,900	1,900	3.30	6.10	6.10
BFB2	17 x 33	140,000	210,000	270	270	2.90	4.00	4.00

2.3 Location of the B-station accelerometer

All the four B-station accelerometers are mounted at the base slab of the building in which they are located. Their position on the base slab is estimated through photos (refer to Appendix I) and it is presented in the Table 2.3.

Table 2.3 Position of the B-stations on the base slab of the building

Station	X_{sensor} [m]	Y_{sensor} [m]
BOWW	2.5	0.2
BAPP	0.2	1.5
BSTD	0.0	4.0
BFB2	0.0	0.0

2.4 Soil profile at the B-station locations

The soil profile characteristics at the B-station location have been estimated based on the closest available CPT-data and are checked based on closest SCPT-data. The resulting soil profiles for the SSI-analysis are reported in Appendix II.

3 RECORDED SIGNAL PROCESSING

All the signals recorded by the B- and G-stations have been collected and analysed such that only those that are reliable are used in the sequel. Table 3.1 presents the number of signals that have been recorded by both B- and G-station for each couple of stations. Table 3.1 also presents the number of signals that were actually further considered in the present analysis after having dropped out the records of poor quality (ref. [3]).

Table 3.1 Number of signals recorded by both B- and G-stations

B-station	Closest G-station	No. recordings	No. recordings after rejecting the problematic
BAPP	G670	10	7
BFB2	G450	15	10
BGAR	G610	6	4
BHAR	G390	11	10
BHKS	G290	2	1
BLOP	G180	12	8
BMD2	G130	5	2
BOWW	G190	10	7
BSTD	G220	13	11
BUHZ	G040	8	5
BWIN	G230	10	8
BWIR	G230	13	11
BWSE	G180	7	6
BZN1	G140	11	3
BZN2	G140	9	4

The FAS ratios between the B- and G-stations have been calculated and are plotted in Figure 3.1 and Figure 3.2. Figure 3.1 presents the B- over G-ratio of the geometric mean of the two horizontal components of all the reliable signals (grey lines) and the average curve of all these signals (blue line). Figure 3.2 presents the B- over G-ratio of the vertical component of all the reliable signals (grey lines) and the average curve of

all these signals (red line). The FAS-ratios calculated are roughly identical to the processing results reported in [1]. Some minor differences are observed, being in some cases attributed to a somewhat different number of event records deemed usable and slight deviations which probably result from noise filtering techniques used.

It is noted that the ratios presented in Figure 3.1 and Figure 3.2 represent the combined result of a number of factors. First, the actual ground motion recorded at a G- and B-station couple (and enters the ratio given below) may be inherently different especially when one focuses at the higher frequencies at which the observed differences are usually larger. Second, the soil conditions may differ between adjacent B- and G-station couples. This is especially true if one considers the scale of variation of the soil conditions compared to the relevant wavelengths of waves for the frequencies of interest. Third, epicentral distances are different as well, and although one may expect this effect to cancel out by considering a large number of recordings at the ratios, one may argue here that this is not the case; certainly not for the induced events, and the magnitudes considered. Finally, differences can be attributed to the effect of the presence of the building in the B-stations which is not there in the G-stations. Given all the factors above, one should be very careful in reaching solid conclusions as to the effects of the building resonances and the degree at which these are expected to be responsible for the major peaks and troughs in the FAS ratio plots. Both average FAS ratios (between B- and G-stations) of the geometric mean horizontal (blue lines) and the vertical component red lines) show these peaks and troughs. In our discussion below, we considered all the factors above in our explanations.

Figure 3.1 FAS ratios of the geometric mean of the horizontal components between B- and G-stations according to Table 3.1. Blue line represents the average of all the reliable recordings (grey lines)

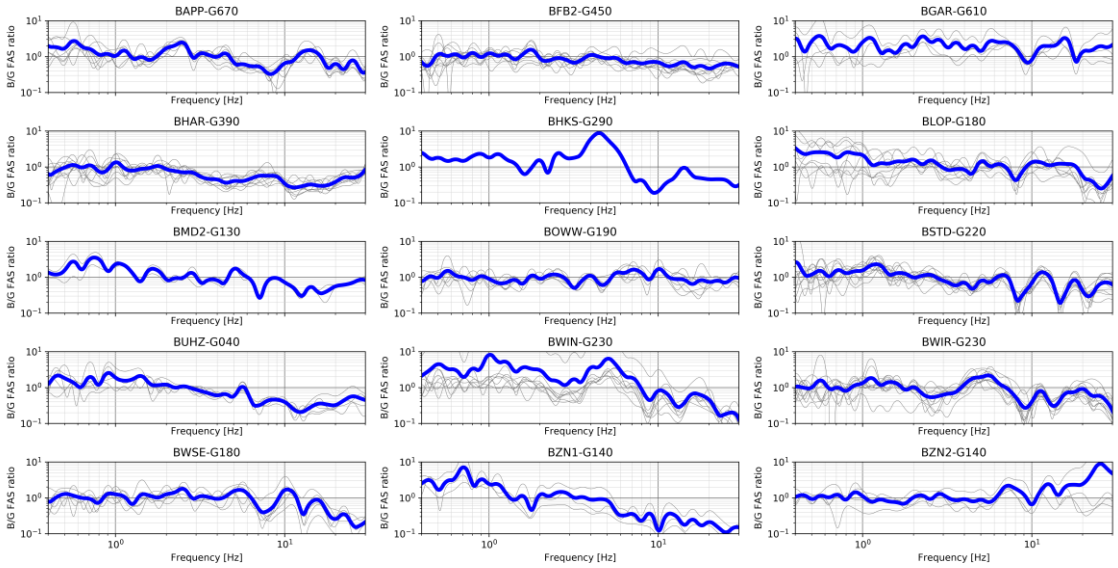

Figure 3.2 FAS ratios of the vertical component between B- and G-stations according to Table 3.1. Red line represents the average of all the reliable recordings (grey lines)

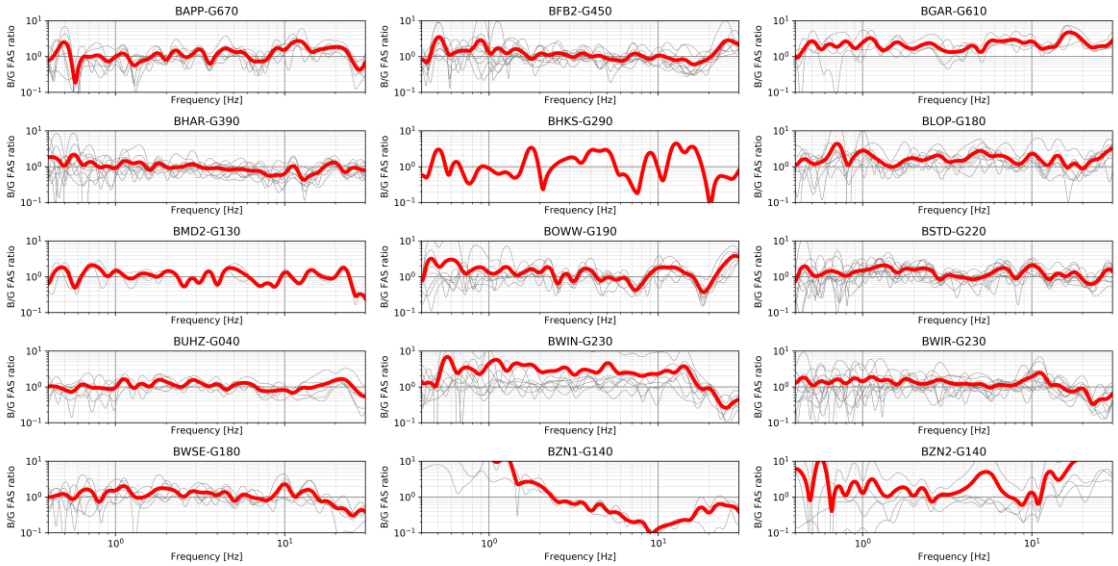

Based on the processed FAS-data and spectrograms that were created for all the records we conclude that we cannot derive any conclusions for frequencies below 2 Hz. The energy of the induced earthquakes in this frequency range is simply very low and signal-to-noise ratio too high to extract useful record data for further analysis.

Some combined B- and G-station couples indicate a decreasing trend of horizontal geometric mean FAS-ratios towards the higher frequencies, which hypothetically could be attributed to kinematic interaction effects. For the vertical direction such a decreasing trend is not observed. Not all horizontal FAS-ratios between close B- and G-station show a clear decreasing trend towards the higher frequencies. Therefore, it cannot be concluded that kinematic interaction effects cause all B-station records to be not useful for ground motion model or ground motion prediction equation development. The B network has the longest operating time and therefore has a major contribution to the total ground motion database. Excluding them all therefore is not recommended.

Among all, the FAS-ratios presented in Figure 3.1 and Figure 3.2, Figure 3.3 and Figure 3.4 focus on the graphs of the four specific study cases chosen in paragraph 2.1.

BOWW - G190 shows, apart from some peaks and troughs, a more or less constant ratio being close to 1.0. No clear decreasing trend towards the higher frequencies is observed. Between the different records quite large variations are observed in the higher frequency range which is absolutely reasonable for all the reasons explained previously. The average ratio approaches 1.0, but per record this is definitely not the case. Higher ratios are calculated around 7 and 10 Hz in the horizontal around 10 Hz for the vertical direction.

BAPP - G670 shows a somewhat decreasing trend towards the higher frequencies, but a major peak is observed for almost all signals around 15 Hz. A clear trough is observed for all signals between 4 and 10 Hz for the horizontal direction. For the vertical direction this is not observed, for which we observe ratios clearly larger than 1.0 for frequencies beyond 10 Hz.

BSTD - G220 clearly shows a decreasing trend towards higher frequencies for the horizontal direction, but very significant consistent peak and troughs are observed. Due to this, the ratio is not below 1.0 at all frequencies, even for the higher ones. The variation between the signals is relatively small for this couple for the horizontal direction. Clearly all the events indicate peaks and troughs for the same frequencies. Peaks are

observed around 7 Hz, 12 Hz, 18 Hz and 24 Hz for the horizontal direction. The vertical direction does not show consistent peaks and troughs for the different events for the horizontal direction and shows ratios on average more or less equal to 1.0 but with large variations among the records for the vertical direction over the total frequency range.

BFB2 - G450 also shows a decreasing trend towards higher frequencies for the horizontal direction, however, in contrast to the previous case, no consistent peaks and troughs are observed as function of frequency. Higher ratios are observed between 4 and 6 Hz approximately. Like for BSTD - G220 also this couple shows for the vertical direction a ratio on average equal to 1.0 over the total frequency range with large variations among the records. A clear peak for between 20 and 25 Hz is observed.

Figure 3.3 FAS ratios of the geometric mean of the horizontal components between B- and G-stations for the four examined case studies. Blue line represents the average of all the reliable recordings (grey lines)

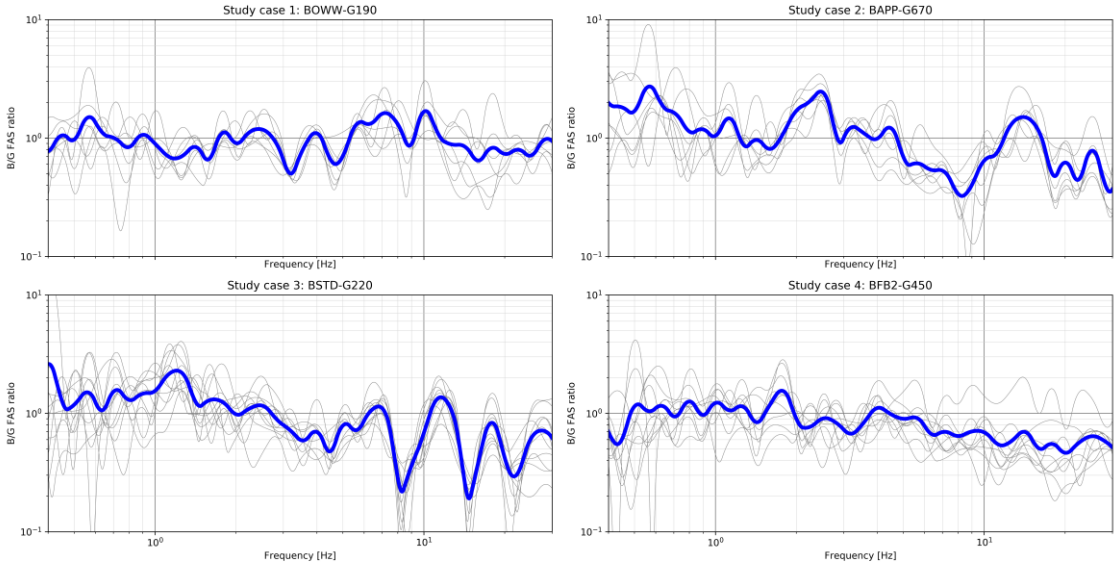

Figure 3.4 FAS ratios of the vertical component between B- and G-stations for the four examined case studies.. Red line represents the average of all the reliable recordings (grey lines)

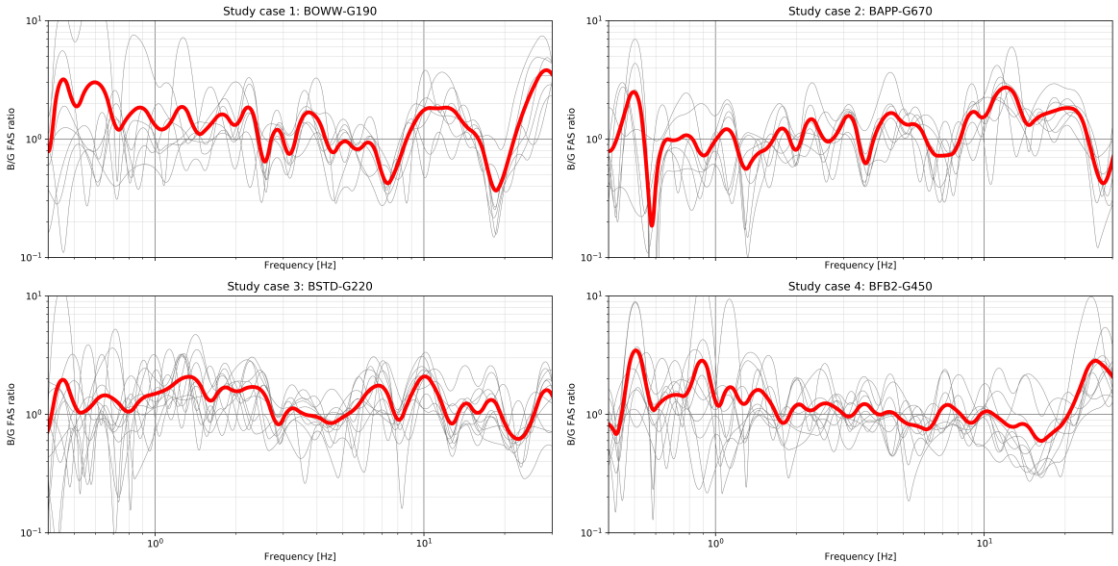

Given that the present study focusses on dynamic amplification functions in the frequency domain PSA ratios are not presented here. PSA ratios are less useful compared to FAS ratios since PSA representation hides a lot of information and sensitivities and will be dominated mainly the superstructures SDOF eigen period.

4 DYNAMIC RESPONSE FUNCTIONS BASED ON NUMERICAL SSI MODELLING

4.1 Soil - structure interaction model

A soil-structure interaction (SSI) model has been developed based on modelling techniques described in ref. [4], [5], [6], [7] and [8]. The building is idealized as described earlier with the properties given in paragraph 2.2. The fully coupled modelling of the combined soil-structure system (illustrated by Figure 4.1) is, in contrary to the building superstructure modelling, not simplistic. The SSI-model involves the following assumptions:

- The base slab of the building is assumed rigid and the connection between the superstructure and the slab is monolithic, i.e. the beam is clamped to the base slab.
- The layered soil profile is generated on the basis of available CPT-data of the closest CPT to the location of each building as described in paragraph 2.4 and Appendix II.
- Uniform incident displacement field is applied at the bottom side of the slab. A unit amplitude has been chosen; since the model a linear scaling factor between the induced motion at the base and the response of the structure applies.
- A frequency sweep, with frequency discretisation of 0.1 Hz, has been applied at all frequencies and for incident ground deformations in the three orthogonal directions.

Figure 4.1 Representation of the modelling of the soil - foundation slab - structure system

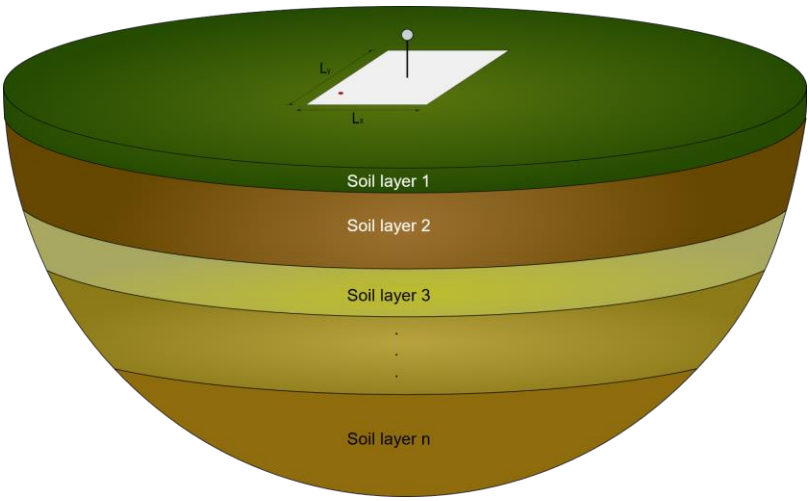

The displacement response is calculated at the position of the sensor. Dynamic response ratios are calculated based on the ratio between the sensor displacement and the incident displacement. Combining the dynamic response ratios over the frequency range results at the so-called frequency dependent dynamic response functions. We present here results in terms of rations between incident displacements and sensor displacement and not in terms of accelerations. The latter are linked to the former by a multiplication factor of ω^2 in the linear regime.

4.2 Calculated dynamic response functions

Figure 4.2 to Figure 4.5 present the results of the numerical modelling. The results are given in terms of displacement response at the position on the base slab where the sensor is located, due to an applied uniform incident displacement at the bottom of the base slab of a unit amplitude.

As a comparison, the displacement response for a G-station slab combined with the B-station soil profile at the middle of a rigid slab due to uniform incident displacement at the bottom of the slab are also plotted in Figure 4.2 to Figure 4.5. These plots replicate the situation of the corresponding G-station given the same soil conditions as at the location B-station.

It is observed that in all cases, the horizontal response calculated at the position of the sensor, due to horizontal uniform unit excitation (response in the same direction as excitation) fluctuates above and below 1.0 at the eigenfrequency of the structure where the B-station is located. This is due to the fact that the system acts as tuned mass damper, reducing the vibration of slab exactly at the first eigenfrequency of the system, i.e. the mass at the top of the beam amplifies its motion while the slab reduces the one of its own The calculated absolute values of the transfer function are highly sensitive to the frequency sweep discretization for such systems with low damping ratios. Therefore, no conclusions should be drawn from the absolute values of the transfer function around this frequency; we are interested only at the location of the peaks of the transfer functions and not at its amplitude to conclude as to the influence on the recorded signals. In all case analysed, it can be seen that uniform unit excitation in any of the two horizontal directions, results in vertical motion of the sensor, mainly around the fundamental eigenfrequency of the building. This effect is caused by the rocking motion of the system. It can be seen that the vertical response due to rocking motion is more significant when the slab is excited in the direction in which the sensor is furthest from the centre of the slab.

The peaks and troughs in the amplification functions in the frequency range around twenty Hz and higher are expected to be caused by the modes of the combined foundation - soil system. This effect is clearly visible from the plots for the horizontal direction, but also applies for the vertical direction were (more gradual) fluctuations are also observed over the total frequency range plotted.

For BSTD (Figure 4.4) a somewhat different pattern is observed for vertical response due to horizontal excitation compared to the others. An interference between structure - foundation rocking and soil continuum seems to cause a less localized amplification function peak over a larger frequency range between three and seven Hz.

Figure 4.2 Displacement response over incident displacement ratio, for the BOWW station case, when the building is present (blue line) and when only a slab of 1.0 m x 2.0 m is considered (replicates situation of a G-station) (red line)

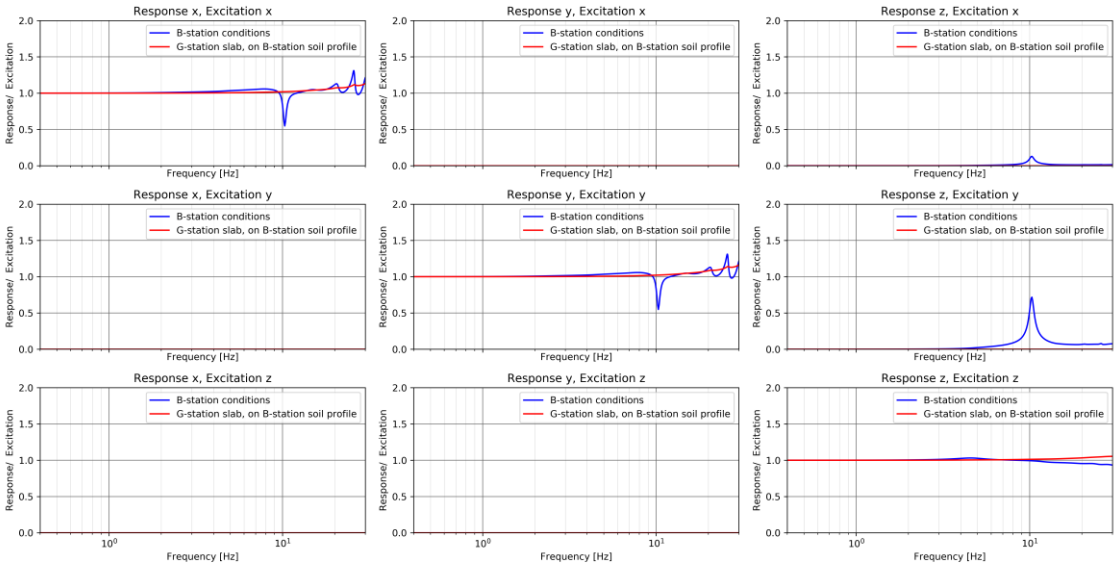

Figure 4.3 Displacement response over incident displacement ratio, for the BAPP station case, when the building is present (blue line) and when only a slab of 1.0 m x 2.0 m is considered (replicates situation of a G-station) (red line)

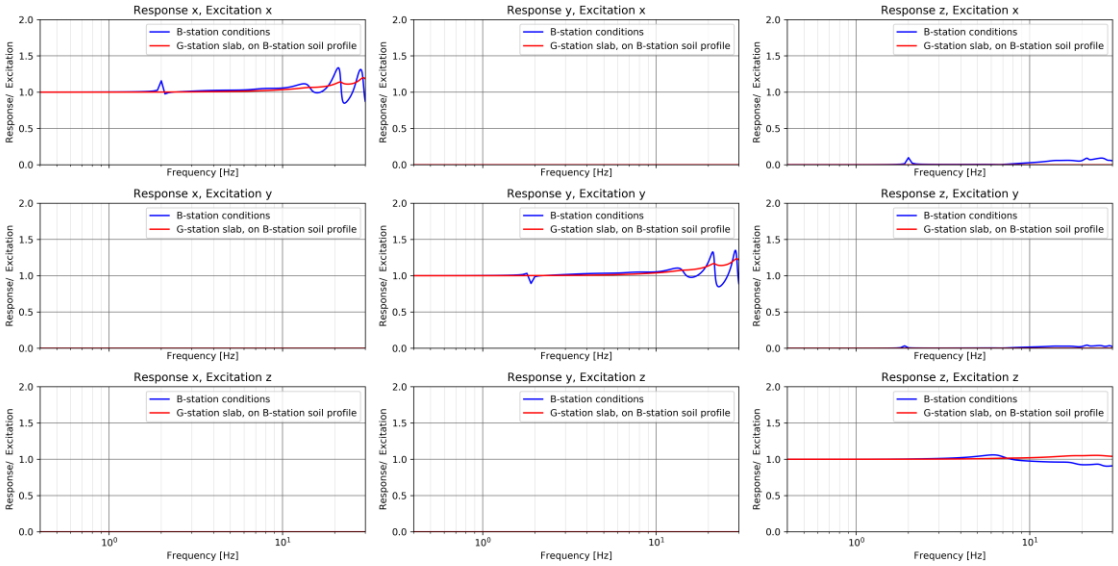

Figure 4.4 Displacement response over incident displacement ratio, for the BSTD station case, when the building is present (blue line) and when only a slab of 1.0 m x 2.0 m is considered (replicates situation of a G-station) (red line)

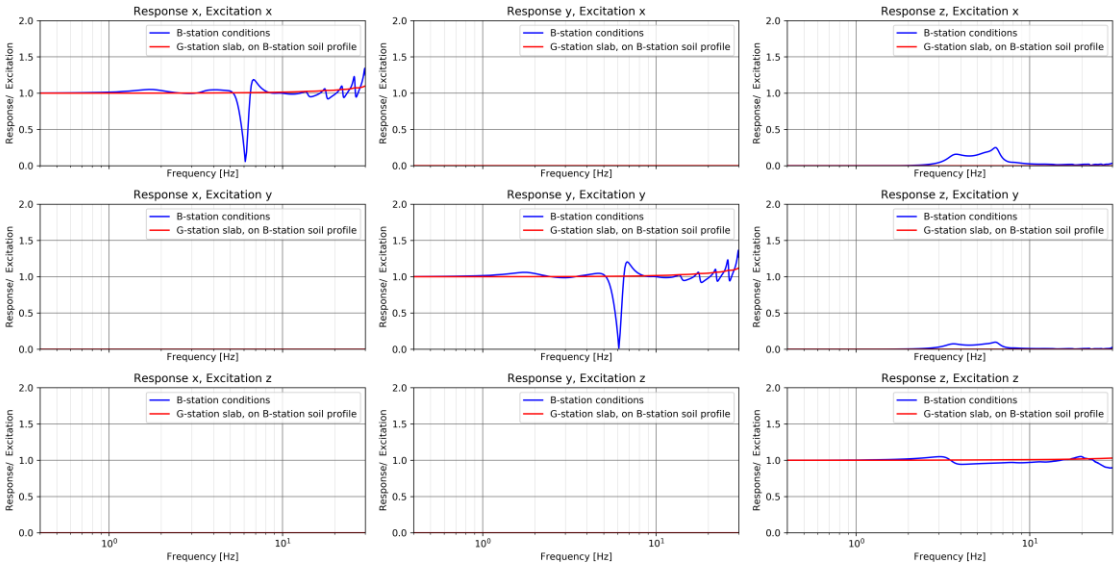

Figure 4.5 Displacement response over incident displacement ratio, for the BFB2 station case, when the building is present (blue line) and when only a slab of 1.0 m x 2.0 m is considered (replicates situation of a G-station) (red line)

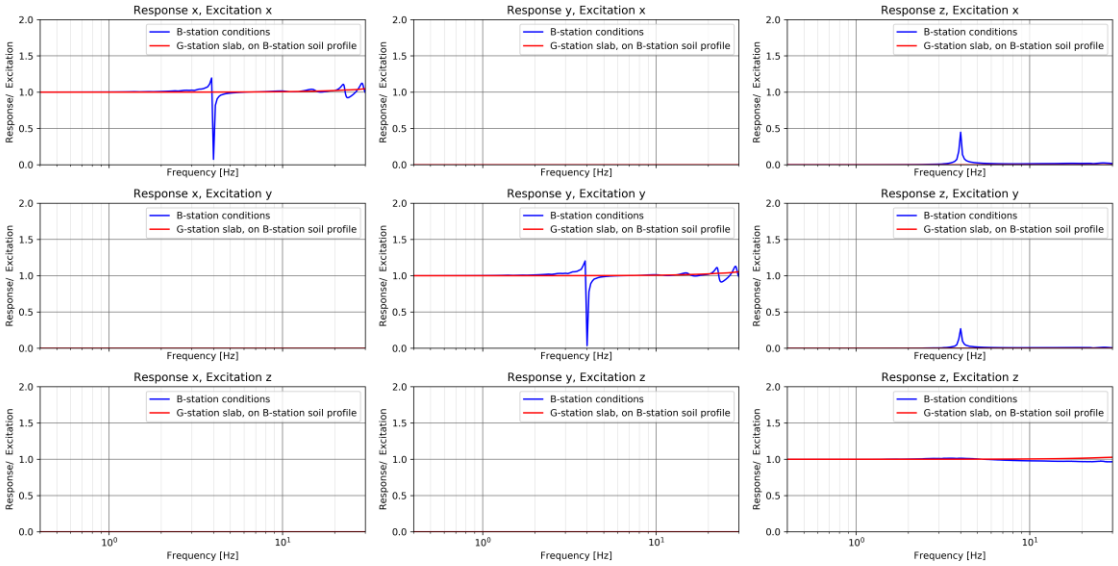

5 ANALYSIS ON THE OBSERVED RECORDS AND NUMERICAL SIMULATION RESULTS

This chapter reports observations that follow form the combined evaluation of the records and the numerical simulations. No repetitive calculations to iterate to better match to the records has been performed. First, this is outside the scope of the present study and would require more information about the B-station buildings and local soil conditions at the location of both B- and G-stations. Second, it is argued that even if we receive a better matching between records and predictions based on the model with the current model this is of little additional value as it adds virtually nothing to the key objective of this study as explained earlier.

Numerical SSI simulations have been performed, which formed the main scope of this project. Moreover, a few linear ground response simulations have been performed in order to be able to better put the SSI-calculation results in perspective to the observed ratios of B-station over G-station records and the possible impact of varying local soil conditions.

5.1 Evaluation of horizontal response

Figure 5.1 shows the station couples horizontal FAS-ratio plots together with the dynamic frequency response functions (FRFs) for horizontal response of the sensor location. Figure 5.2 shows the B-station FAS-plots together with the FRFs for horizontal response of the sensor location on the foundation slab. It can be concluded that are resonances in the relevant frequency range. These resonances can be attributed to modes of vibration of the coupled soil-structure system that involve a large amplification of the response of the top mass. These resonances are characterised by low damping and thus the dynamic amplification concentrates at relatively narrow frequency bands. Combined analysis of FAS and SSI-amplification functions show that in terms of absolute motion amplitude the impact of inertial SSI-effects on building horizontal response limited. No clear effect on the FAS-amplitude near the SSI-system first resonance frequency is observed. This may be explained by the very short duration ground motion, which may not activate such effects in the frequency range of interest (SSI-fundamental mode frequencies range from two to ten Hz).

Figure 5.1 Average FAS ratios of the geometric mean of the horizontal components between B- and G-stations for the four examined case studies (blue lines) and calculated displacement response over incident displacement ratio in x-direction (red lines) and y-direction (green lines)

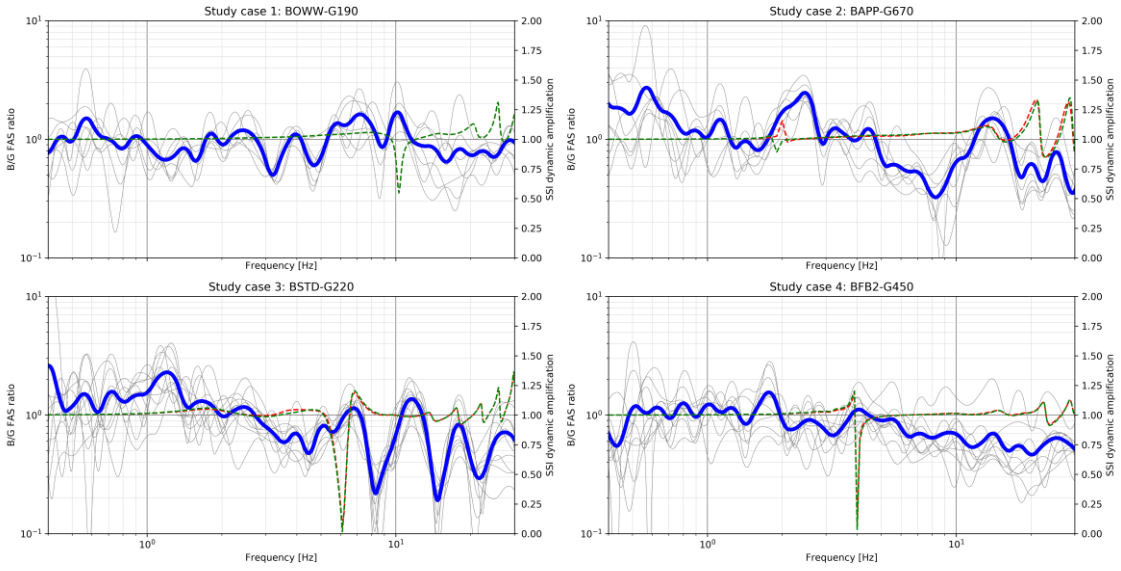

Figure 5.2 Average FAS of the geometric mean of the horizontal components of B-stations for the four examined case studies (blue lines) and calculated displacement response over incident displacement ratio in x-direction (red lines) and y-direction (green lines)

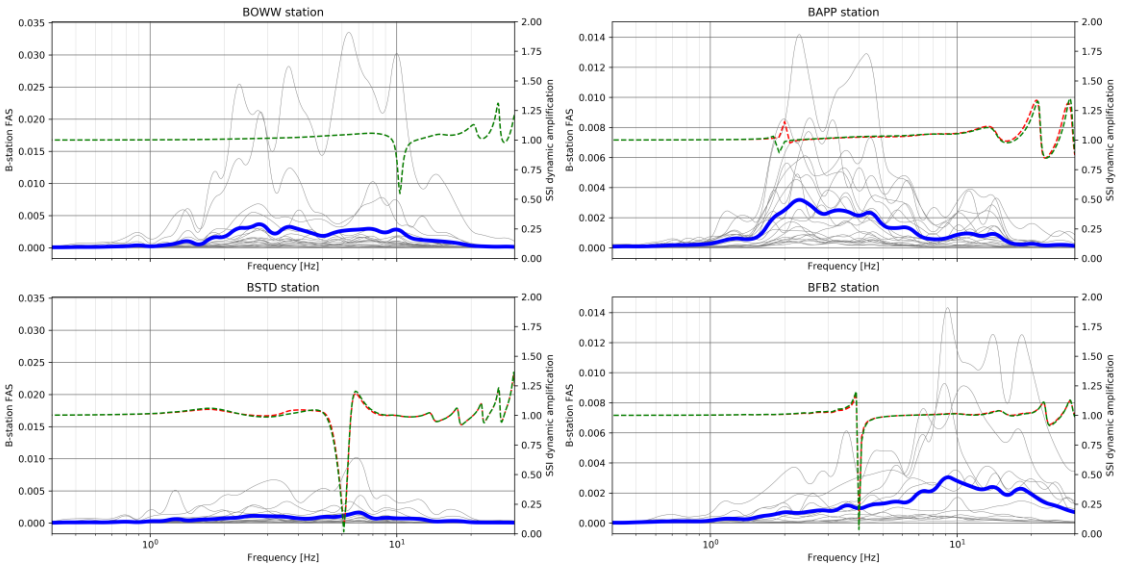

Since no clear effects could attributed to the influence of the dynamic building response and dynamic SSI (often referred to in codes as 'inertial SSI effects'), the potential impact of varying soil conditions has been studied by a number of linear elastic ground response analysis. Moreover, it has been evaluated if code-based correction factors for kinematic SSI-effects (non-synchronous base excitation caused by the different arrival times of the waves at different locations below the foundation) are capable to explain the observed deviations between B-station and G-station records.

Transfer functions of horizontal ground response for vertically propagation S-waves are plotted with the horizontal geometric mean FAS of the records in Figure 5.3. The legends for the ground response transfer functions shown in the plots refer to the corresponding CPT-names from the NAM-database. For BOWW and BAPP stations the transfer functions peaks seem to match the peaks of the FAS of the recorded motions. In the frequency range below 2 Hz no match is observed, which probably is caused by low frequency content of the ground motion in this frequency range. No consistent pattern between the ground response transfer function and the recorded ground motion is observed for stations BSTD and BFB2.

Figure 5.3 Average FAS of the geometric mean of the horizontal components of B-stations for the four examined case studies (blue lines) and calculated ground response transfer function for nearby CPTs (red and green lines)

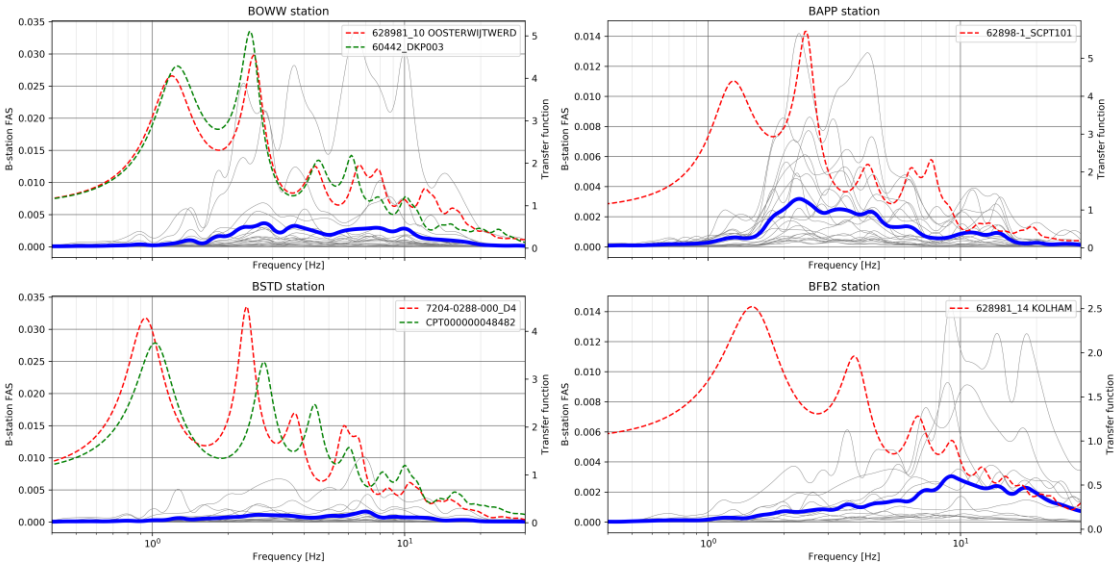

Ground response analysis have not been performed for the G-stations because no detailed soil profile data were available in these locations. For some the CPT being closest to the coupled B-station would also be the closest for the G-station, but with quite a larger CPT-station distance. From the ground response analysis, it can be concluded that soil profiles derived based on 'close' CPTs show a clear shift in the dynamic amplification function peaks. By comparing the variation in the transfer functions for ground response to the FRFs, we conclude that the effect of different site conditions is most likely larger than the impact of the structure-foundation system in this case.

Aiming for further explanation of the observed reduced B-station horizontal recordings for higher frequencies the NEHRP-provisions for response spectrum reduction due to kinematic effects (base slab averaging and embedment effects) according to ref. [9] and ref. [10] have been implemented. According to NEHRP the kinematic effects can be corrected for by a frequency dependent factor that transforms response spectra calculated for actual ground motions into reduced response spectra calculated for building foundation motions. The functional form can be found in ref. [9] and ref. [10]. Figure 5.4 shows the results of this implementation and its comparison to the ratios calculated for the four couples of B- and G-stations selected for the present study. Please note that SA-ratios and not FAS-ratios are presented in this figure. In the calculated correction factors a modification compared to the NEHRP-formula has been implemented to correct for typically higher frequency content of Groningen ground motions and soft soil conditions in Groningen. This adjustment would need to be substantiated further based on further research.

The comparison in Figure 5.4 can be concluded to show a very consistent trend between recorded ratios and ratios predicted according to NEHRP. The trend shows a decrease beyond a frequency around three Hz and a more or less constant ratio towards the larger frequencies. The peaks and troughs that vary per station couple cannot be explained by kinematic effects and are most likely explained by site amplification effects. An integration of the kinematic effect correction with differences in site response effects may further improve the accuracy of the correction factors. This can be done when G-stations SCPT-results become available.

Figure 5.4 Calculated PSA ratios for the four selected station couples (blue) compared to the NEHRP code-based PSA ratios (red)

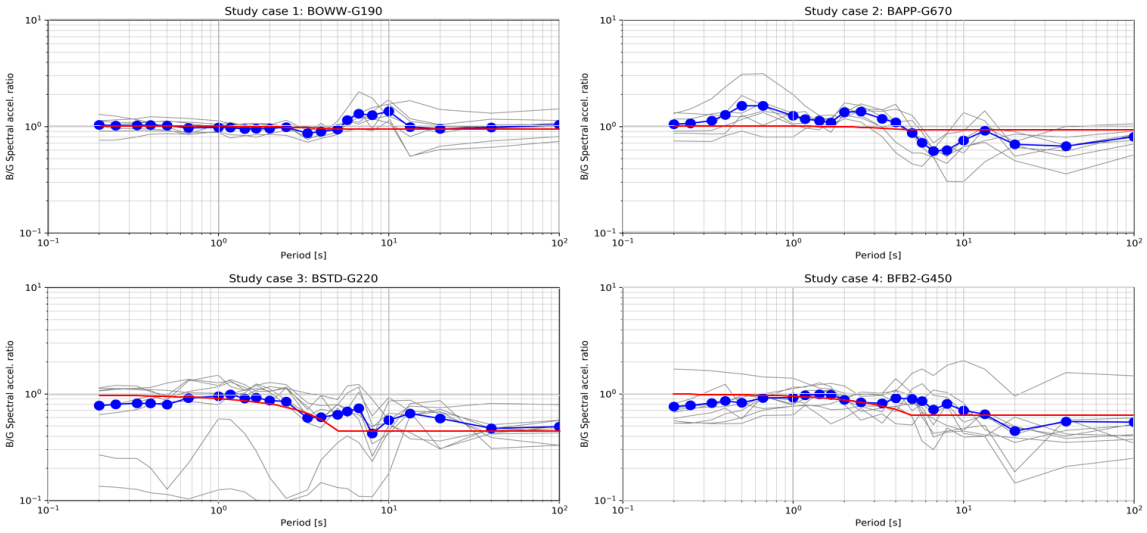

5.2 Evaluation of vertical response

Figure 5.5 shows the station couples vertical FAS ratio plots together with the FRFs for the vertical response of the sensor. Figure 5.6 shows the B-station vertical FAS together with the FRFs. In terms of absolute value of the transfer functions (which relates to steady state response), a significant amplification effect (both vertical and rocking) is shown. This, however, is not so clearly observed from the vertical FAS of the records. It is hypothesised that the duration of excitation by the seismic signal is too short to trigger a state of resonance which is significant in comparison to the amplitude of the vertical ground motion dominated by P-waves. This becomes also very clear form the time-frequency analysis of some records of significant events that have been recorded at the studied B-stations (included in Appendix III). In these spectrograms, the highest intensity of the vertical component motion is clearly concentrated at the start of the event when P-waves arrive at the station location. However, it is seen that there is some influence of the building response in this case at the relevant frequency range for some of the station couples which can be attributed to building resonance which is not fully developed due to the short duration of the ground motion excitation and/or the insignificant amount of energy in the signal at the correspondent frequencies.

Figure 5.5 Average FAS ratios of the vertical component between B- and G-stations for the four examined case studies (solid red lines), calculated vertical displacement response, due to: vertical incident displacement (red dashed lines), horizontal incident displacement in x-direction (blue dashed lines), horizontal incident displacement in y-direction (black dashed lines) and algebraic sum of the later 3 (green lines)

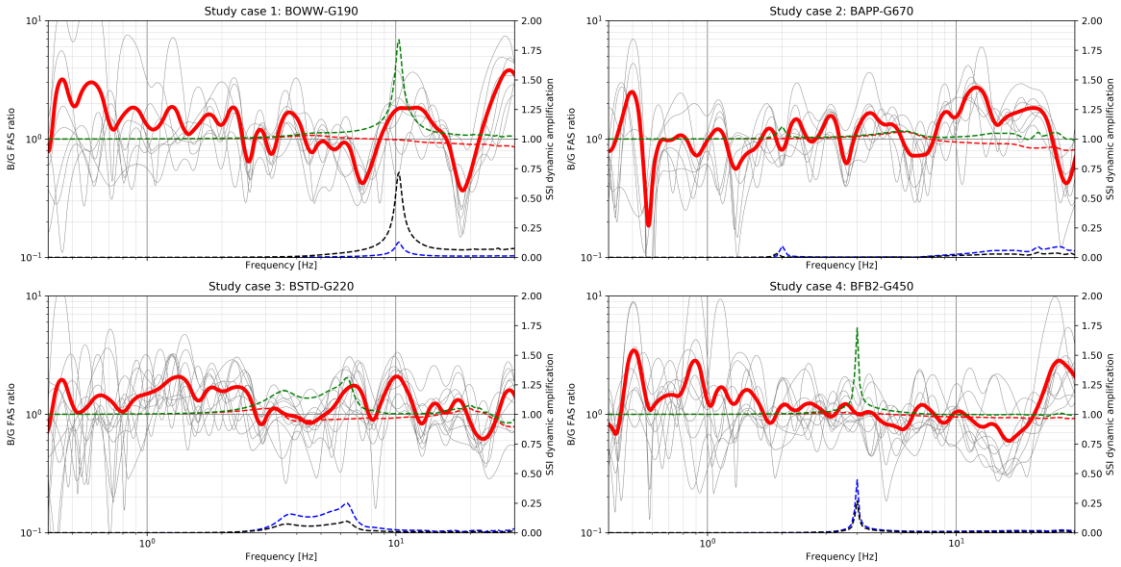

Figure 5.6 Average FAS of the vertical component between B- and G-stations for the four examined case studies (solid red lines), calculated vertical displacement response, due to: vertical incident displacement (red dashed lines), horizontal incident displacement in x-direction (blue dashed lines), horizontal incident displacement in y-direction (black dashed lines) and algebraic sum of the later 3 (green lines)

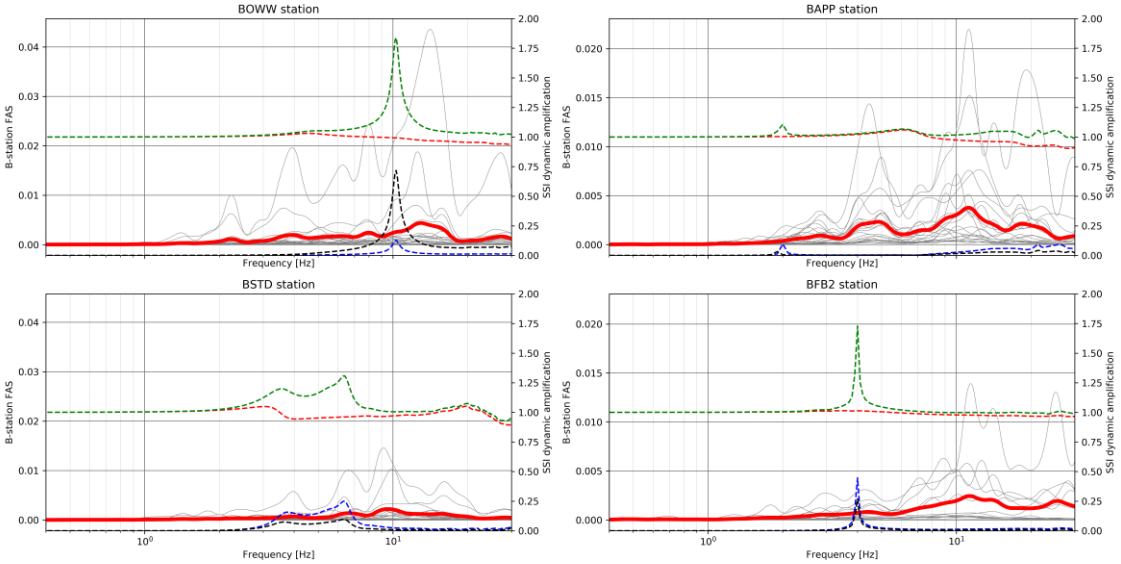

6 CONCLUSIONS AND RECOMMENDATIONS

6.1 Conclusions

Analysis of the horizontal geometric mean FAS of B- and G-station records shows a decreasing trend towards the higher frequencies, especially for the larger buildings. Analysis of the vertical FAS ratios of B-stations relative to close by G-stations results in no clear decreasing trend of B- relative to G-stations records towards the higher frequencies. Four pairs of close by B- and -stations (BOWW-G190, BAPP-G670, BSTD-G220, BFB2-G450) have been selected with the objective to increase understanding in the relative contribution of inertial soil-structure interaction (de)amplification effects on B-station response.

The superstructure has been described with a reduced-order model which is coupled to layered soil continuum in an advanced semi-analytical formulation including dynamic soil-structure interaction (SSI). Numerical simulations of the fully coupled superstructure-foundation-soil system have been performed. A uniform incident ground motion has been applied and the foundation slab motion at the location of the B-station accelerometer has been calculated. From the analysis it is concluded that:

- Resonances of the coupled superstructure-foundation-soil system in the relevant frequency range are possible and cannot be excluded. Such resonance effects are concentrated usually to narrow frequency bands when they involve motions of the coupled system in which the mass of the building structure resonates with high amplitude.
- Combined analysis of FAS and spectrograms (time-frequency representation of the records) and FRFs show that the although the effect of the building in the response at the location of the sensor is expected to be limited this cannot be excluded a priori. This due to the fact that different events may generate different ground motions and, for some of them, resonance of the building is possible at the higher frequency range. However, the duration of the seismic events in Groningen is short and therefore this resonance will also be limited in time and not-fully developed. For stronger events though, this situation may alter. More specifically:
    - For the vertical ground motions, the arrival of the early P-waves may yield some resonance behaviour of the building at the higher frequencies. However, this is limited due to the short duration of the signals analysed so far and, in any case, the amplification shown in some B-stations at these frequencies cannot be attributed solely to this factor.
    - For the horizontal ground motions, the sensitivity of the FAS of the records to the ground response transfer function seems to dominate over the amplification that may be caused by resonances of the coupled superstructure-foundation-soil system.

In conclusion, one can say that the combined analysis of ground motion recordings in terms of energy content at various frequencies shows that the Groningen ground motions have significant energy at frequencies at which the coupled superstructure-foundation-soil system may resonate. However, the strong ground motion duration (at least for the events considered thus far) relative to the time needed for the resonance to develop at the examined frequency ranges is simply too short. Thus, resonance may develop in some cases and this may influence the recordings at the B-stations, however, this cannot be seen as a general trend.

6.2 Recommendations

Some combined B- and G-station couples indicate a decreasing trend of horizontal geometric mean FAS ratios towards the higher frequencies, which hypothetically could be attributed to kinematic interaction effects. For the vertical direction such a decreasing trend is not observed. Not all horizontal FAS ratios between close B- and G-station show a clear decreasing trend towards the higher frequencies. Moreover, no decrease for the vertical component is observed at all. Therefore, it cannot be concluded that kinematic interaction effects disqualify all B-stations from being useful for the development of ground motion prediction equations. Based on an evaluation of the FAS ratio plots and the building typologies it can be

concluded that such effects are most pronounced for the larger/heavier and/or piled buildings (BUHZ, BFB2, BHAR, BHKS, BMB2, BSTD, BZN1).

Directly comparing B- to G-stations involves many (unknown) parameters that could cause different patterns of ground motions. Preliminary analysis on the potential impact of realistic soil profile variations based on nearby CPT indicates that the effect of soil profile variations could be very significant as well. Since no soil profile data is available for the G-stations it was impossible to evaluate to what extend this has affected the observed B- to G-station FAS-ratios. Doing so after the planned G-station ground survey data becomes available would probably lead to more solid conclusions with respect to the deviations observed between the B- to G-station records.

Kinematic effects is the often-used terminology for SSI-effects related to 'non-synchronous base excitation' caused by the different arrival times of the waves at different locations below the foundation. In contrast to resonances associated with coupled superstructure-foundation-soil system in which the building mainly resonates, kinematic interaction effects result a more uniform effect on FAS-amplitudes. Typically a more or less linearly increasing reduction factor beyond a threshold frequency and a constant ratio for high frequencies is observed for kinematic effects (base slab averaging and embedment effects) If these effects could be well understood and quantified given the specific conditions at all B-station locations, one could possibly retrieve equivalent ground motions from B-station records. The comparison of recorded ratios to modified code-based corrections for kinematic interaction as shown in Figure 5.4 indicates that code-based corrections predict very well the observed trends. The attempt made includes a modification based on the hypothesis that Groningen records typically show higher frequencies and soil conditions are less stiff in Groningen. Further substantiation of the modifications made to the code-based correction factors would be necessary. It is however concluded that first result indicates a high level of predictability of the kinematic effects. Moreover, it is expected that integration with correction factors for site amplification could further improve the quality of the explanation for deviations in B-station horizontal recordings. These elements are recommended for further study. The B network has the longest operating time and therefore has a major contribution to the total ground motion database. Excluding it altogether is therefore not recommended from many perspectives.

7 REFERENCES

[1] Seister, Analysis of consistency between B- and G-stations records for induced events in the Groningen gas field., Draft Report, Document No. STR_FUG_18P17_01, d.d. 19 April 2019.

[2] Crowley, H., and Pinho, R., Report on the v5 Fragility and Consequence Models for the Groningen Field, November 2017.

[3] Witteveen+Bos, (2019), Investigation of malfunctioning earthquake recording stations for Groningen Earthquake events of the period 2014-2018, Staatstoezicht op de Mijnen, ref 113982/19-005.563, draft version 01.

[4] Tsouvalas, A., De Oliveira Barbosa, J., & Lourens, E-M. (2017). Validation of a coupled FE-BE model of amasonry building with in-situ measurements. In 16th World Conference on Earthquake Engineering (16WCEE 2017) [4892] The Institute of Theoretical and Applied Mechanics.

[5] Oliveira Barbosa, J. M. and Kausel, E. (2012), The thin-layer method in a cross-anisotropic 3D space. Int. J. Numer. Meth. Engng, 89: 537-560. doi:10.1002/nme.3246

[6] Oliveira Barbosa, J.M., Park, J. and Kausel, E. (2012), Perfectly matched layers in the thin layer method, Computer Methods in Applied Mechanics and Engineering, vol 217-220, p.p 262-274.

[7] Kausel, E., Roësset, J.M., (1981), Stiffness matrices of layered soils, Bulletin of the Seismological Society of America, vol 71(6), p.p. 1743-1761.

[8] Kausel, E., (2006), Fundamental Solutions in Elastodynamics, A compendium, Cambridge University Press, doi:10.1017/CB09780511546112.

[9] NIST GCG 12-917-21, Soil-Structure Interaction for Building Structures, NEHRP Consultants Joint Venture, September 2012.

[10] FEMA440, Improvement of Nonlinear Static Seismic Analysis Procedures, NEHRP, June 2005.

APPENDIX: SDOF EQUIVALENT PROPERTIES OF THE SUPERSTRUCTURES FOR THE SELECTED B-STATIONS

I.1 Case study 1: BOWW ( )

Global dimensions

The design drawings that we have received for the building (dated on 1977) are clearly outdated, because the wooden shed in which the BOWW station is located (based on photos), has not been built that long ago. For this reason, we will estimate the dimensions and the characteristics of the building purely based on the photos.

The plan dimensions of the wooden shed have been measured through the QGIS software approximately to be equal to 6.0 m by 6.0 m (refer to Figure I.1). This corresponds well with the right photo of, in which we counted around 42 vertical wooden planks. Assuming that each plank is around 15 cm, 42*15 = 6.3 m.

Figure I.1 Dimensions of the wooden shed where the BOWW station is located from QGIS

Figure I.2 Wooden shen in which the BOWW-station is located

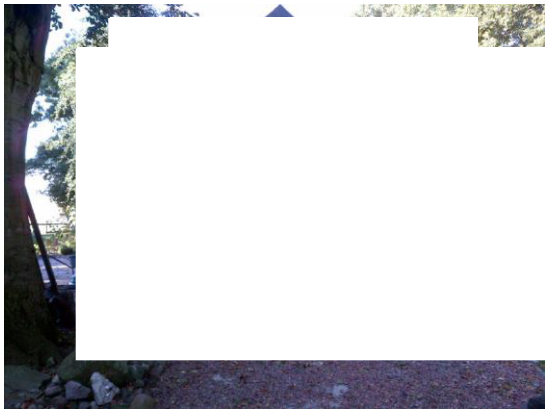

Foundation slab

The foundation is assumed to be a concrete slab without piles, 100 mm thick. Assuming a density of 2,500 kg/m^3, this results in a mass of:

$$6 \times 6 \times 0.1 \times 2500 = 9{,}000 \text{ kg}$$

Location of station

Judging by the photos of Figure I.1 and Figure I.2 the station is assumed to be located 0.2 m from the wall and 0.5 m from the middle line of the foundation slab (refer to Figure I.1).

Figure I.1 Location of the antenna of the BOWW-station outside of the wooden shed

Figure I.2 Location of the BOWW-station inside the wooden shed

Figure I.3 Location of BOWW station on the foundation slab

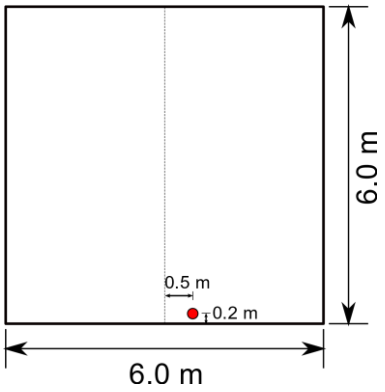

Superstructure SDOF system

The mass calculation is summarized as follows:

Columns

Columns are assumed to be 150×150 mm. Available photo material does not show the number (or dimensions) of the columns, so 8 columns are assumed. This results in a volume of:

$$8 \times 0.15^2 \times 2.40 = 0.432 \text{ m}^3$$

Sheeting

It is assumed that the sheeting is a single layer of 18 mm. This results in a volume of:

$$(4 \times 6 \times 2.40) \times 0.018 = 1.037 \text{ m}^3$$

Bracings

Based on Figure I.1 bracings are assumed to be 100×40 mm. Available photo material does not show the number (or dimensions) of the columns, so 2 bracings per wall are assumed. Additionally, assuming that the bracings are in an angle of 60° this results in a volume of:

$$4 \times 2 \times 0.1 \times 0.04 \times \frac{2.40}{\sin 60} = 0.089 \text{ m}^3$$

Figure I.1 Bracing in the wooden shed where BOWW is located

Total volume of timber (for the equivalent beam) is then:

$$0.432 + 1.037 + 0.089 = 1.558 \text{ m}^3$$

The type of timber elements is unknown, so an average type of hardwood is selected. Assuming a strength class of D30, the mean density is 630 kg/m^3. The total mass of the timber is then:

$$1.558 \times 630 = 981.5 \text{ kg}$$

Which corresponds to the following mass per meter of the equivalent beam of 2.4 m:

$$981.5/2.4 = 410 \text{ kg}$$

The stiffness calculation is summarized as follows:

Columns

For the columns, the following dimensions and conditions are assumed:

Cross section	$A = 150 \times 150$ mm
height	$l = 2{,}400$ mm
Boundary conditions	Clamped at top and bottom
Young's modulus	$E = 11{,}000 \text{ N/mm}^2$ (D30)
Moment of inertia	$I = 1/12\, bh^3 = 42{,}187{,}500 \text{ mm}^4$

Assuming that the roof is acting as a diaphragm, meaning that the top of the columns is not allowed to rotate, the lateral stiffness per column is estimated by:

$$\frac{12EI}{l^3} = \frac{12 \times 11{,}000 \times 42{,}187{,}500}{2400^3} = 402.8 \text{ N/mm} = 400{,}800 \text{ N/m}.$$

Bracings

For the braces, the following dimensions and conditions are assumed:

Cross section	$A = 100 \times 40$ mm
height	$l = 2{,}770$ mm
inclination	$\theta = 60°$
Boundary conditions	Hinged at top and bottom
Young's modulus	$E = 11{,}000$ N/mm^2 (D30)

The axial stiffness is:

$$k_{axial} = \frac{EA}{L} = 15{,}900 \text{ N/mm}.$$

The lateral stiffness:

$$k_{lateral} = k_{axial} \times \cos^2\theta = 3{,}975{,}000 \text{ N/m}.$$

Available photos do not show the exact layout or number of columns and braces. Therefore, 8 columns and 4 braces are assumed. Hence, the total stiffness is estimated to be:

$$k = 8 \times 400{,}800 + 4 \times 3{,}975{,}000 = 19.1 \times 10^6 \text{ N/m}.$$

Assuming that the beam of the equivalent SDOF is clamped both at the top and at the bottom (roof behaves as diaphragm), the EI of the beam will be:

$$k = \frac{12EI}{h^3} \rightarrow EI = \frac{k \times h^3}{12} = \frac{19.1 \times 10^6 \times 2.4^3}{12} = 22 \text{ MN}m^2$$

The lumped mass calculation is summarized as follows:

Beams

Beams are assumed to be 200×80 mm. Photos show multiple beams spanning across the width of the building, except for the first 2 meters, near the door opening. Assuming 500 mm spacing between beams, this results in 15 beams of 5m length. Additionally, 3 beams of 8.5 m are assumed over the length of the building. This results in a volume of:

$$15 \times 0.20 \times 0.08 \times 5 \; + \; 3 \times 0.20 \times 0.08 \times 8.5 \; = 1.608 \text{ m}^3.$$

Rafter

8 rafters are assumed in the roof with the same dimensions as the beams. This results in a volume of:

$$8 \; \times 0.20 \times 0.08 \times 3.90 = 0.499 \text{ m}^3.$$

Sheeting

Assuming that the height of the roof is 3 m and the same sheets are used as for the walls of the shed the volume is:

$$(2 \times \frac{1}{2} \times 6 \times 3) \times 0.018 = 0.324 \text{ m}^3.$$

Roof

Assuming that the roof is made of roofing tiles, the weight of the roof is estimated to be 48 kg/m^2. The total weight of the roof is then:

$$4{,}24 \times 6 \times 2 \times 48 = 2{,}444 \text{ kg}.$$

Assuming the same type of wood as for the walls of the structure the lumped mass is equal to:

$$M = (1.608 + 0.499 + 0.324) \times 630 + 2{,}444 = 4{,}000\text{kg}$$

I.2 Case study 2: BAPP (Appingedam)

Global dimensions

The width and length of the wooden shed (5.0 x 8.5 m) and the height of the gutter (2.4 m) are presented in the received drawings (refer to Figure I.1).

Figure I.1 Drawings of the wooden shed where the BAPP-station is located

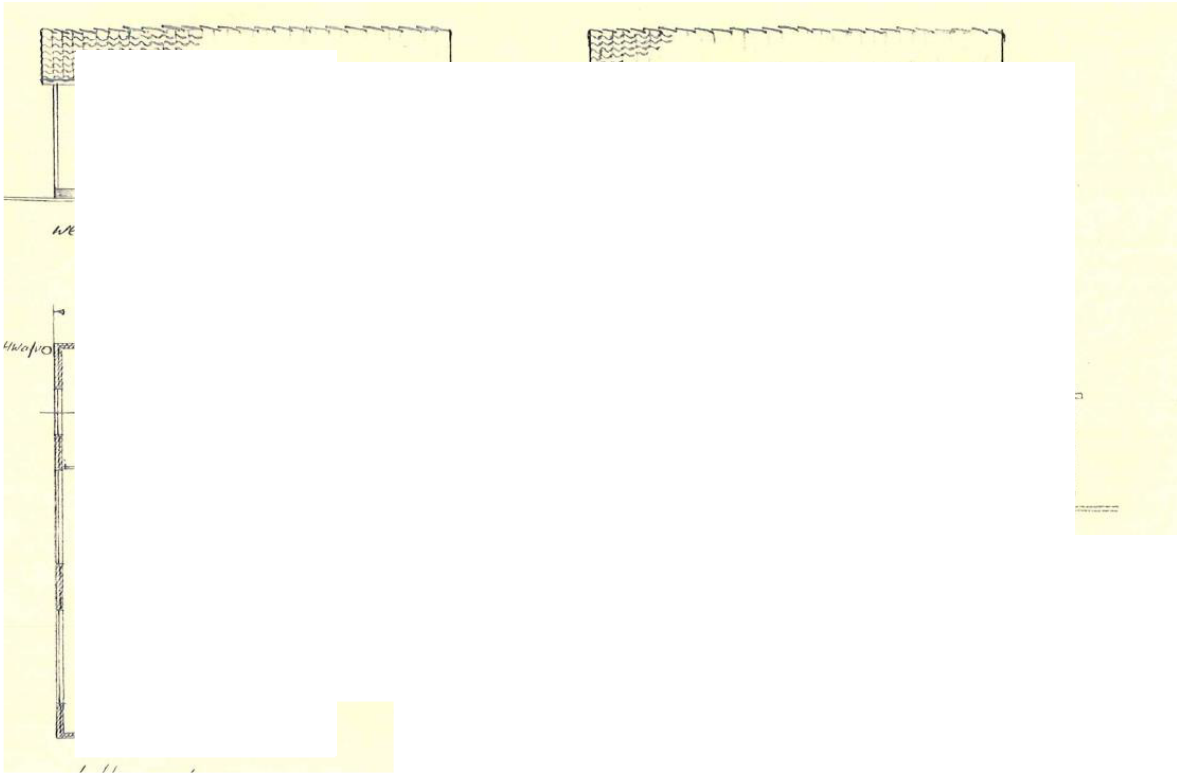

Foundation slab

The foundation is assumed to be a concrete slab without piles, 100 mm thick. Assuming a density of $2{,}500\ \mathrm{kg/m^3}$, this results in a mass of:

$$5 \times 8.5 \times 0.1 \times 2500 = 10{,}625\ \mathrm{kg}$$

Location of station

Judging by the photos of Figure I.1 and Figure I.2 the station is assumed to be located 0.2 m from the wall and 0.5 m from the middle line of the foundation slab (refer to Figure I.3).

Figure I.1 Location of the antenna of the BAPP-station outside of the wooden shed

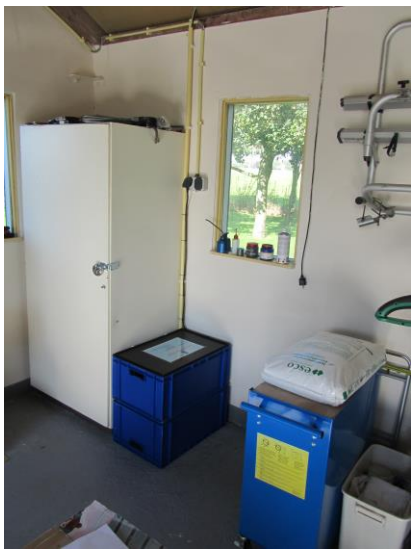

Figure I.2 Location of the BAPP-station inside the wooden shed

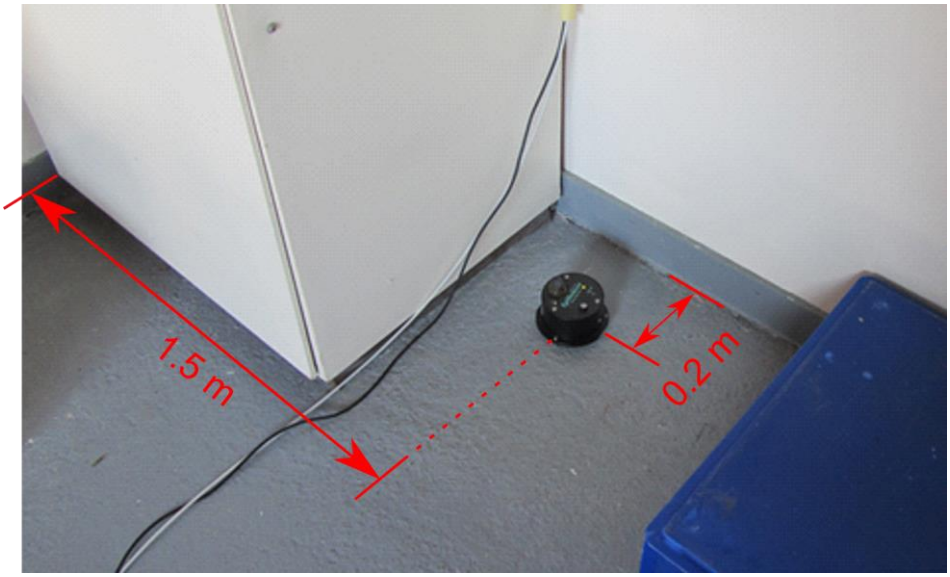

Figure I.3 Location of BAPP-station on the foundation slab

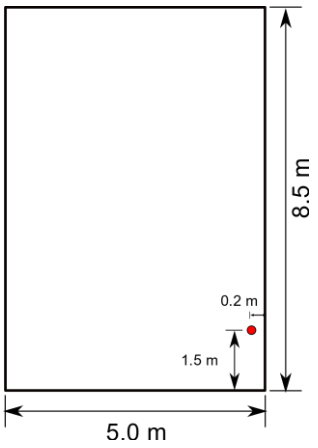

Superstructure SDOF system

The mass calculation is summarized as follows:

Columns

Columns are assumed to be 100×100 mm. Drawings (refer to Figure I.1) show 27 columns. This results in a volume of:

$$27 \times 0.10^2 \times 2.40 = 0.648 \text{ m}^3.$$

Sheeting

Drawings show that walls are composed out of two timber leaves of 18 mm. Assuming that timber runs around the entire building, this results in:

$$(2 \times 5 \times 2.40 + 2 \times 8.5 \times 2.40) \times 2 \times 0.018 = 2.333 \text{ m}^3.$$

Total volume of timber (for the equivalent beam) is then:

$$0.648 + 2.333 = 2.981 \text{ m}^3.$$

The type of timber elements is unknown, so an average type of hardwood is selected. Assuming a strength class of D30, the mean density is 630 kg/m^3. The total mass of the timber is then:

$$2.981 \times 630 = 1{,}878 \text{ kg}.$$

Stucco

The stucco on the walls is estimated to be 5 mm thick on each side, with a density of $2{,}300$ kg/m^3. Assuming that it is applied on all sides of the building, neglecting doors and windows, the added mass is:

$$(2 \times 5 \times 2.40 + 2 \times 8.5 \times 2.40) \times 0.01 \times 2{,}300 = 1{,}490 \text{ kg}.$$

Thus, the mass per length of height of the equivalent column is (1,878+1,490)/2.4 = 1,400 kg/m.

The stiffness calculation is summarized as follows:

Columns

For the columns, the following dimensions and conditions are assumed:

Cross section	$A = 100 \times 100$ mm
height	$l = 2{,}400$ mm
Boundary conditions	Clamped at top and bottom
Young's modulus	$E = 11{,}000$ N/mm^2 (D30)
Moment of inertia	$I = 1/12\, bh^3 = 8.33 \times 10^6$ mm^4

Assuming that the roof is acting as a diaphragm, meaning that the top of the columns is not allowed to rotate, the lateral stiffness per column is estimated by:

$$\frac{12EI}{l^3} = \frac{12 \times 11{,}000 \times 8.33 \times 10^6}{2{,}400^3} = 79.54 \text{ N/mm} = 79{,}540 \text{ N/m}.$$

Sheeting

The way in which the sheeting has been placed (vertical planks between two wooden columns, approximately 1 m far from each other, (refer to Figure I.1) provides an additional shear stiffness to the building. Assuming the following characteristics for the shedding conditions are assumed:

Cross section	$A = 1{,}000 \times 36$ mm
height	$l = 2{,}400$ mm
Shear modulus	$G = 780$ N/mm^2 (GL28H)

Hence, the shear stiffness provided by each assembly is:

$$\frac{GA}{l} = \frac{780 \times 36{,}000}{2{,}400} = 11.7 \text{ N/mm} = 11{,}700 \text{ N/m}.$$

Figure I.1 shows that the building has 13 sheeting assemblies in the longitudinal and 5 in the transverse direction. Taking into account 27 columns with square cross-section that provide the same flexural stiffness in both lateral directions, the stiffness in the two direction is estimated:

$$k_{longitudinal} = 27 \times 19{,}885 + 13 \times 11{,}700 = 6.9 \times 10^5 \text{ N/m}$$
$$k_{transverse} = 27 \times 19{,}885 + 5 \times 11{,}700 = 6.0 \times 10^5 \text{ N/m}$$

Assuming that the beam of the equivalent SDOF is clamped both at the top and at the bottom (roof behaves as diaphragm), the EI of the beam will be:

$$k = \frac{12EI}{h^3} \rightarrow EI = \frac{k \times h^3}{12}$$

$$EI_{longitudinal} = \frac{k \times h^3}{12} = \frac{6.9 \times 10^5 \times 2.4^3}{12} = 7.95 \times 10^5$$

$$EI_{transverse} = \frac{k \times h^3}{12} = \frac{6.0 \times 10^5 \times 2.4^3}{12} = 6.90 \times 10^5$$

The lumped mass calculation is summarized as follows:

Beams
Beams are assumed to be 100×100 mm. Photos and drawings don't show much information about the beams, so 3 beams of 8.5 m are assumed over the length of the building. This results in a volume of

$$3 \times 0.10 \times 0.10 \times 8.5 \ = 0.255 \ \mathrm{m}^3$$

Sheeting
Drawings (refer to Figure I.1) so that the height of the roof is 1.1 m and the same sheets are used as for the walls of the shed. Then the volume is:

$$(2 \times \frac{1}{2} \times 5 \times 1.1) \times 0.018 = 0.1 \ \mathrm{m}^3$$

Rafter
No rafters are visible in the photos or drawings. However, 8 rafters are assumed in the roof with the same dimensions as the beams. This results in a volume of:

$$8 \ \times 0.10 \times 0.10 \times 2.73 = 0.218 \ \mathrm{m}^3$$

Total volume of timber is then:

$$0.255 + 0.1 + 0.218 = 0.573 \ \mathrm{m}^3$$

The type of timber elements is unknown, so an average type of hardwood is selected. Assuming a strength class of D30, the mean density is $630 \ \mathrm{kg/m}^3$. The total mass of the timber is then:

$$0.573 \times 630 = 360 \ \mathrm{kg}$$

Roof
Assuming that the roof is made of roofing tiles, the weight of the roof is estimated to be $48 \ \mathrm{kg/m}^2$. The total weight of the roof is then:

$$2.73 \times 8.50 \times 2 \times 48 = 2{,}228 \ \mathrm{kg}$$

Total lumped at the roof mass is then:

$$360 + \ 2{,}228 = 2{,}600 \ \mathrm{kg}$$

I.3 Case study 3 BSTD (Stedum)

Global dimensions

The estimation of the mass, the stiffness and the gutter height of the barn in which the BSTD station is located will be done by comparing the footprint of this barn to the most similar index building in the v5 fragility and consequence models report (refer to [2]). This turns to be the De Haver index building with the following characteristics:
Effective mass: 745,000 kg
Effective height: 3.3 m
Footprint: 1,530 + 194 = 1,724 m^2
1st Eigen-period: 0.164 s

The width and length of the barn in which the BSTD station is located is estimated through the QGIS software approximately equal to 40.0 m by 25.0 m (refer to Figure I.1).

Figure I.1 Dimensions of the barn where the BSTD station is located from QGIS

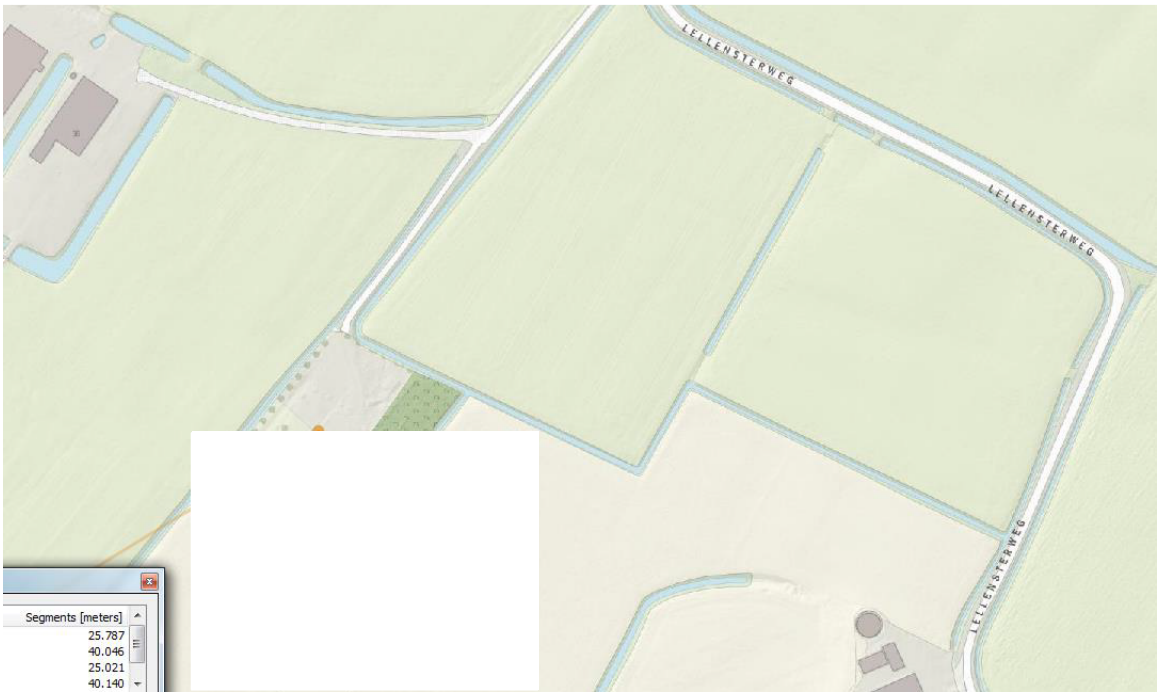

Foundation slab

The foundation is assumed to be a concrete slab without piles, 100 mm thick. Assuming a density of $2500\ \mathrm{kg/m^3}$, this results in a mass of:

$$40 \times 25 \times 0.1 \times 2500 = 250{,}000\mathrm{kg}$$

Location of station

Judging by the photos of Figure I.1 and Figure I.2 the station is approximately be located 4.0 m from the corner of the barn in the longitudinal direction (refer to Figure I.3).

Figure I.1 Approximate indication of the location of the BSTD

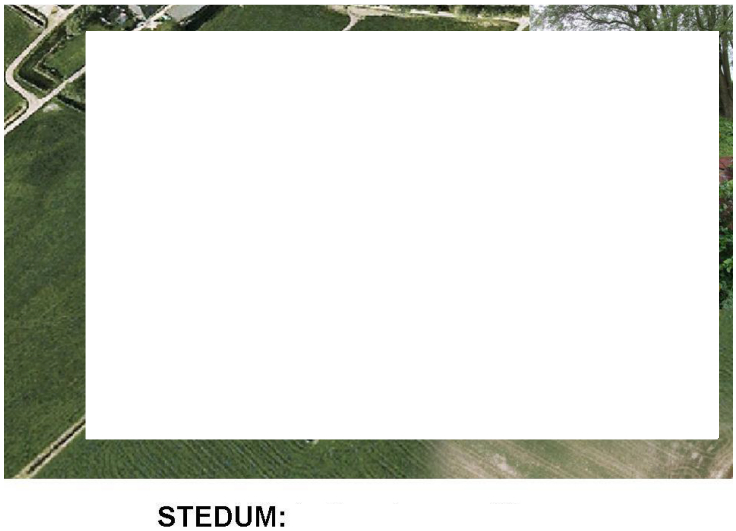

Figure I.2 Location of the BSTD station inside the barn.

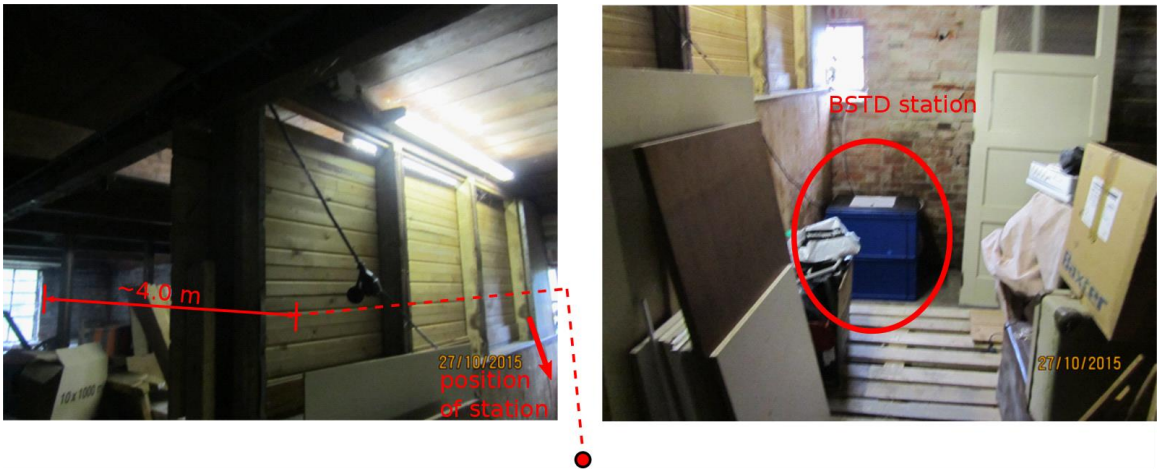

Figure I.3 Location of BSTD station on the foundation slab

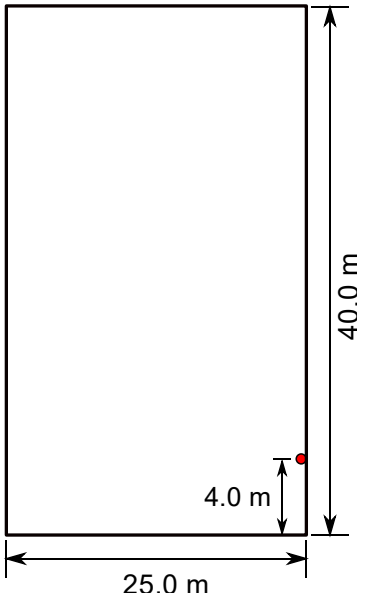

Superstructure SDOF system

The mass calculation is summarized as follows:

Due to lack of details it is assumed that the whole mass of the building is been transferred partially to the top and partially at the base slab. Therefore, no weight per height of the equivalent beam is calculated.

The stiffness calculation is summarized as follows:

The lateral stiffness of the equivalent SDOF system in the case of this barn is not calculated directly. It is assumed that the barn in which the BSTD station is located, is expected to have similar eigen period as the De Haver index building, which is 0.164 s. Hence, the stiffness is:

$$k = 4 \times \frac{m \times \pi^2}{T_{De\ Haver}^2} = 4 \times \frac{432{,}000 \times \pi^2}{0.164^2} = 6.34 \times 10^8 \text{ N/m}$$

Assuming that the beam of the equivalent SDOF is clamped both at the top and at the bottom (roof behaves as diaphragm), the EI of the beam will be:

$$k = \frac{12EI}{h^3} \rightarrow EI = \frac{k \times h^3}{12}$$

$$EI_{longitudinal} = \frac{k \times h^3}{12} = \frac{6.34 \times 10^8 \times 3.3^3}{12} = 1.9 \times 10^9$$

The lumped mass calculation is summarized as follows:

The mass of the barn is calculated indirectly by comparing its relative size with index building De Haver in the v5 fragility and consequence models report.

The estimated area of the barn is 25×40 m, compared to 1,724 m^2 for the Haver. The mass is therefore estimated as:

$$M_{BSTD} = \frac{A_{BSTD}}{A_{De\ Haver}} \times M_{De\ Haver} = \frac{25 \times 40}{1{,}724} \times 745{,}000 = 432{,}000 \text{ kg}$$

I.4 Case study 4 BFB2 (Kolham)

Global dimensions

The estimation of the mass, the stiffness and the gutter height of the barn in which the BFB2 station is located will be done by comparing the footprint of this barn to the most similar index building in the v5 fragility and consequence models report (refer to [2]). This turns to be the De Haver (no house) index building with the following characteristics:

Effective mass: 576,000 kg
Effective height: 2.9 m
Footprint: 1,530 m^2
1st Eigen-period: 0.25 s

The width and length of the barn in which the BFB2 station is located is estimated through drawings (refer to Figure I.1) equal to 33 m by 17 m.

Figure I.1 Drawing of the barn where the BFB2 station is located

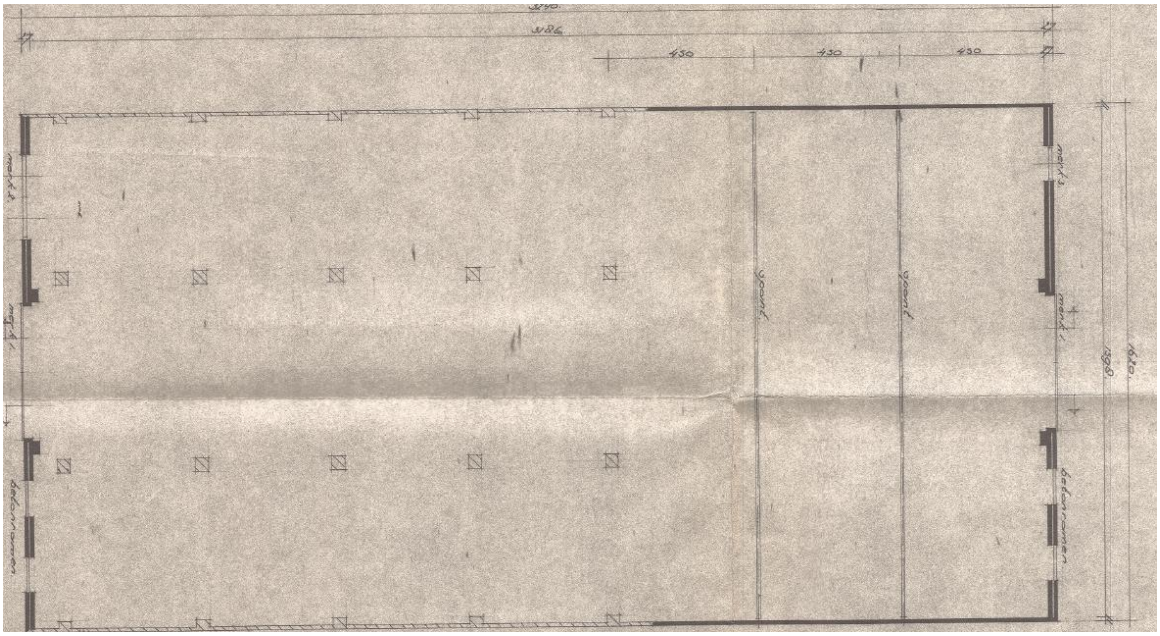

Foundation slab

The foundation is assumed to be a concrete slab without piles, 100 mm thick. Assuming a density of $2{,}500\ \mathrm{kg/m^3}$, this results in a mass of:

$$33 \times 17 \times 0.1 \times 2{,}500 = 140{,}000\mathrm{kg}$$

Location of station

Judging by the photo of Figure I.1 the station is at a corner of the barn (refer to Figure I.2).

Figure I.1 Location of the BFB2 station inside the barn

Figure I.2 Location of BFB2 station on the foundation slab

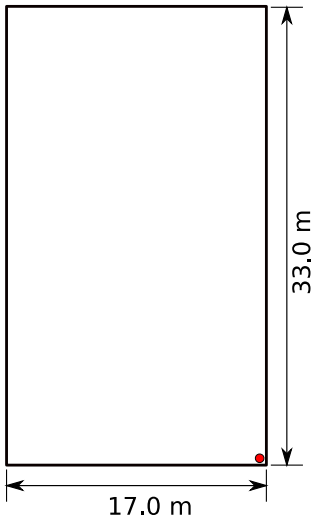

Superstructure SDOF system

The mass calculation is summarized as follows:

Due to lack of details it is assumed that the whole mass of the building is been transferred partially to the top and partially at the base slab. Therefore, no weight per height of the equivalent beam is calculated.

The stiffness calculation is summarized as follows:

The lateral stiffness of the equivalent SDOF system in the case of this barn is not calculated directly. It is assumed that the barn in which the BSTD station is located, is expected to have similar eigen period as the De Haver (no house) index building, which is 0.25 s. Hence, the stiffness is:

$$k = 4 \times \frac{m \times \pi^2}{T_{De\ Haver}^2} = 4 \times \frac{210{,}000 \times \pi^2}{0.25^2} = 1.33 \times 10^8 \text{ N/m}$$

Assuming that the beam of the equivalent SDOF is clamped both at the top and at the bottom (roof behaves as diaphragm), the EI of the beam will be:

$$k = \frac{12EI}{h^3} \rightarrow EI = \frac{k \times h^3}{12}$$

$$EI_{longitudinal} = \frac{k \times h^3}{12} = \frac{1.33 \times 10^8 \times 2.9^3}{12} = 2.7 \times 10^8$$

The lumped mass calculation is summarized as follows:

The mass of the barn is calculated indirectly by comparing its relative size with index building De Haver in the v5 fragility and consequence models report.

The estimated area of the barn is 17×33 m, compared to 1,530 m^2 for the Haver. The mass is therefore estimated as:

$$M_{BSTD} = \frac{A_{BSTD}}{A_{De\ Haver}} \times M_{De\ Haver} = \frac{17 \times 33}{1{,}530} \times 576{,}000 = 210{,}000 \text{ kg}$$

APPENDIX: SOIL CONDITIONS AT B-STATION LOCATIONS

The soil conditions for the B-station locations are determined based on closest available CPT data from the Groningen CPT database received from NAM. In addition, they have been checked based on the closest available SCPT V_s data. A visualisation of the CPT data and the corresponding resulting soil profiles for SSI analysis are reported below.

B-station BAPP

CPT S07F00311.csv has been used.

Figure II.1 CPT data available closest to BAPP and estimated shear wave velocity based on correlation

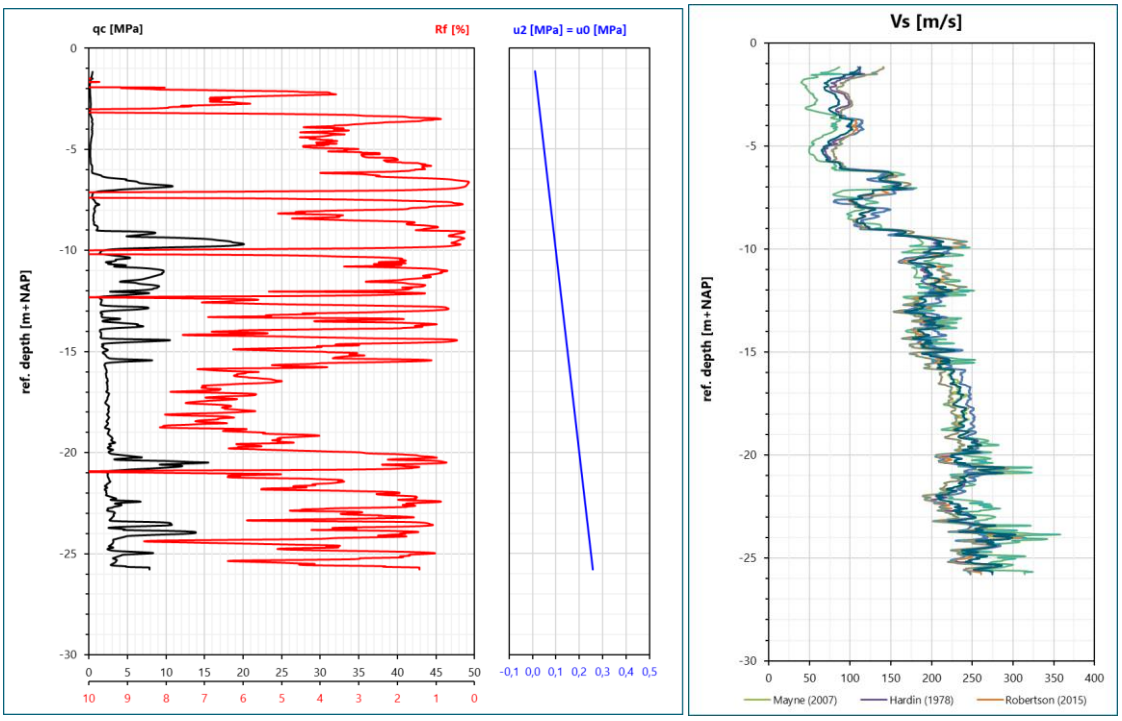

Table II.1 Soil profile schematization BAPP

Layer	Depth NAP [m]	Saturated unit weight [kN/m^3]	Vs [m/s]	Soil type
1	-1 to -6	16.0	85	clay, silty clay
2	-6 to -7	20.0	175	sand
2	-7 to -9	17.0	120	clayey silt, sandy silt
3	-9 to -12	19.5	200	sandy silt, silty sand, some clay lenses
4	-12 to -20	19.0	235	clay
5	-20 to -21	19.5	275	sand
6	-21 to -23	19.0	235	clay, sand lenses
7	-23 to -26	19.0	275	clay, sand lenses

No information is available below NAP -26 m. Based on the global Groningen geological model this will be either pot clay or sand. A shear wave velocity equal to V_s = 300 m/s and saturated unit weight 20 kN/m^3 have been assumed.

B-station BFB2

CPT 628981_14_KOLHAM.csv has been used.

Figure II.2 CPT data available closest to BFB2 and estimated shear wave velocity based on correlation

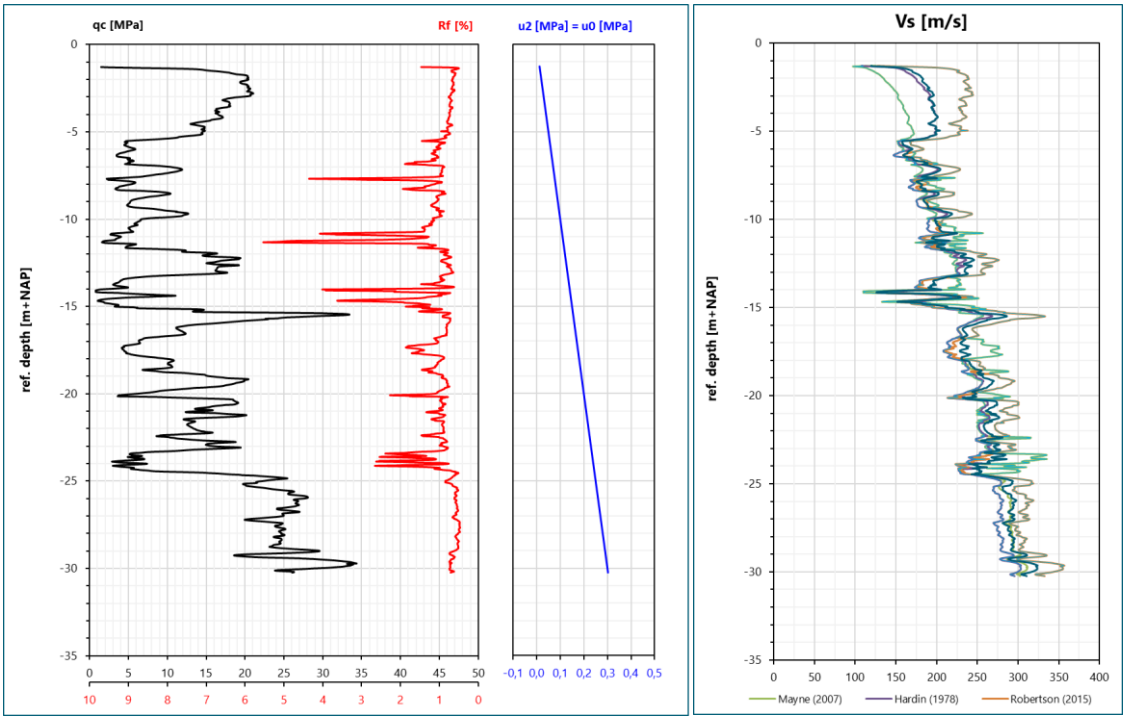

Table II.2 Soil profile schematization BFB2

Layer	Depth NAP [m]	Saturated unit weight [kN/m^3]	Vs [m/s]	Soil type
1	-1 to -5.5	20	190	sand
2	-5.5 to -10	19	175	sand, clay lenses
3	-10 to -12	16	200	clay, organic
4	-12 to -13.5	20	225	sand
5	-13.5 to -15	16	175	clay, organic
6	-15 to -23.5	20	250	sand, clay/silt lenses
7	-23.5 to -24.5	17.5	225	clay
8	-25 to -30	20.5	300	sand

No information is available below NAP -30 m. It has been assumed that the Pleistocene sand layer can be continued down to deeper depths for the SSI calculations.

B-station BOWW

CPT 628981_10 O D.csv has been used.

Figure II.3 CPT data available closest to BOWW and estimated shear wave velocity based on correlation

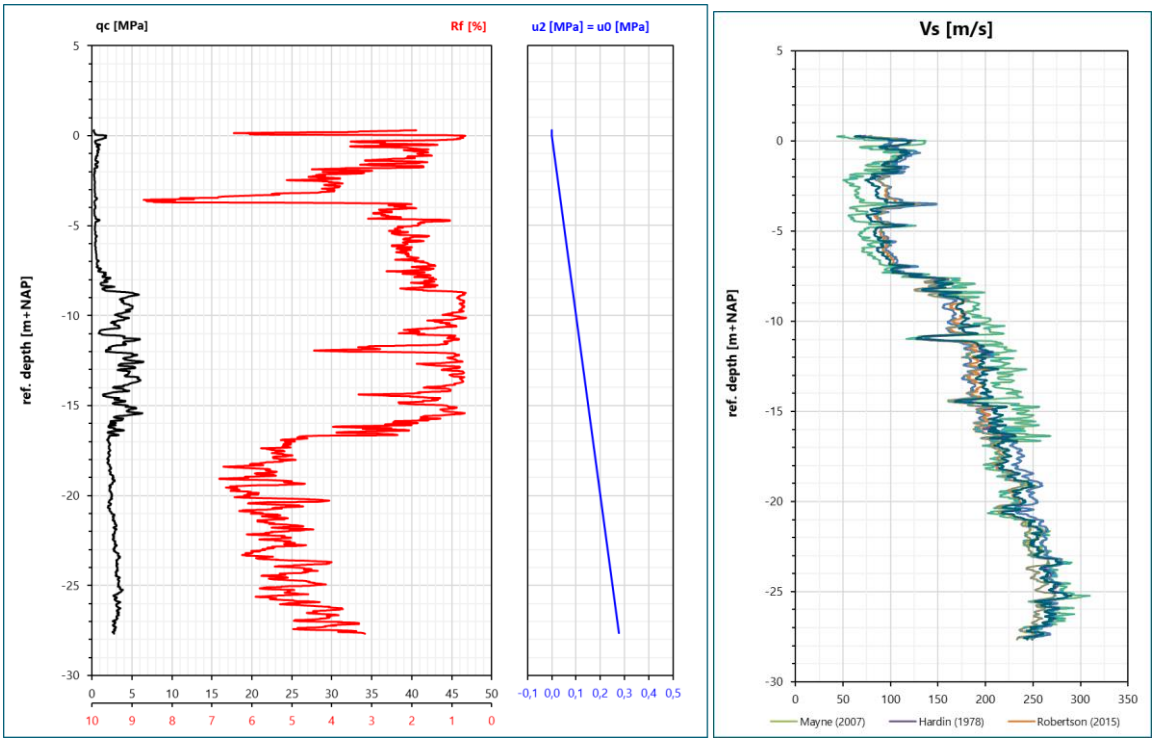

Table II.3 Soil profile schematization BOWW

Layer	Depth NAP [m]	Saturated unit weight [kN/m^3]	Vs [m/s]	Soil type
1	0.5 to -2	17	110	silty clay or mixed top layer
2	-2 to -4	15	85	clay, organic
3	-4 to -8.5	16	100	clay, silty clay
4	-8.5 to -10.5	18	175	sandy silt or sand with clay lenses
5	-10.5 to -12	16.5	150	clay
7	-12 to -14	18.5	200	sandy silt
	-14 to -15	16.5	175	clay
8	-15 to -16	18.5	210	sandy silt
9	-16 to -21	18.5	225	pot clay
10	-21 to -28	18.5	275	pot clay

No information below NAP -28 m. It has been assumed that pot clay continues, with slightly increasing stiffness with depth, which for our purpose can be assumed to be constant.

B-station BSTD

CPT CPT00000048482.csv and 7204-0288-000_D4.csv have been used. The soil profile schematization has been based on two CPTs because of the limited exploration depth of the CPT closest to the B-station.

Figure II.4 CPT data available closest to BSTD and estimated shear wave velocity based on correlation

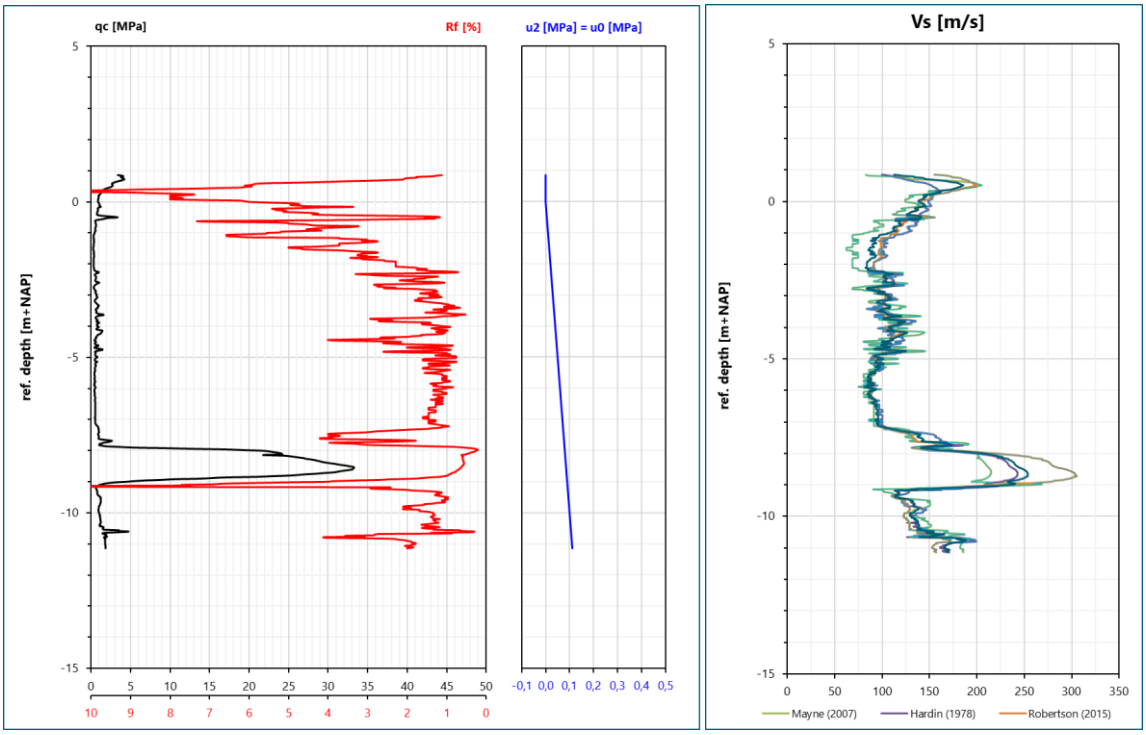

Table II.4 Soil profile schematization BSTD

Layer	Depth NAP [m]	Saturated unit weight [kN/m^3]	Vs [m/s]	Soil type
1	1 to -0.5	18.5	125	anthropogenic top layer / mixture of sands / clays
2	-0.5 to -3	14	75	organic clay or peat
3	-3 to -7.5	15	90	soft clay with sand lenses
4	-7.5 to -10.5	16	100	organic clay
5	-10.5 to -13	20	235	clean sand
6	-13 to -14	18	150	sand mixtures
7	-14 to -15	20	210	clean sand
	-15 to 16	18	175	sand mixtures
7	-16 - -17	20	240	clean sand
8	-17 - -19	18.5	210	pot clay

Below NAP -19 m pot clay has been assumed based on the global Groningen geological model. The stiffness has been assumed to be increasing with depth. Subsequent layers of ~5 m thickness with constant but increasing stiffness, ending up at around 280 to 300 around 30 m depth, have ben modelled in SSI calculations.

APPENDIX: ACCELERATION TIME SERIES, SPECTROGRAMS AND FAS AND SNR PLOTS OF STRONGEST EVENTS WITH SMALL EPICENTRAL DISTANCE TO THE STUDIES B-STATIONS

Figure III.1 BOWW - Zeerijp 2018 (5 km)

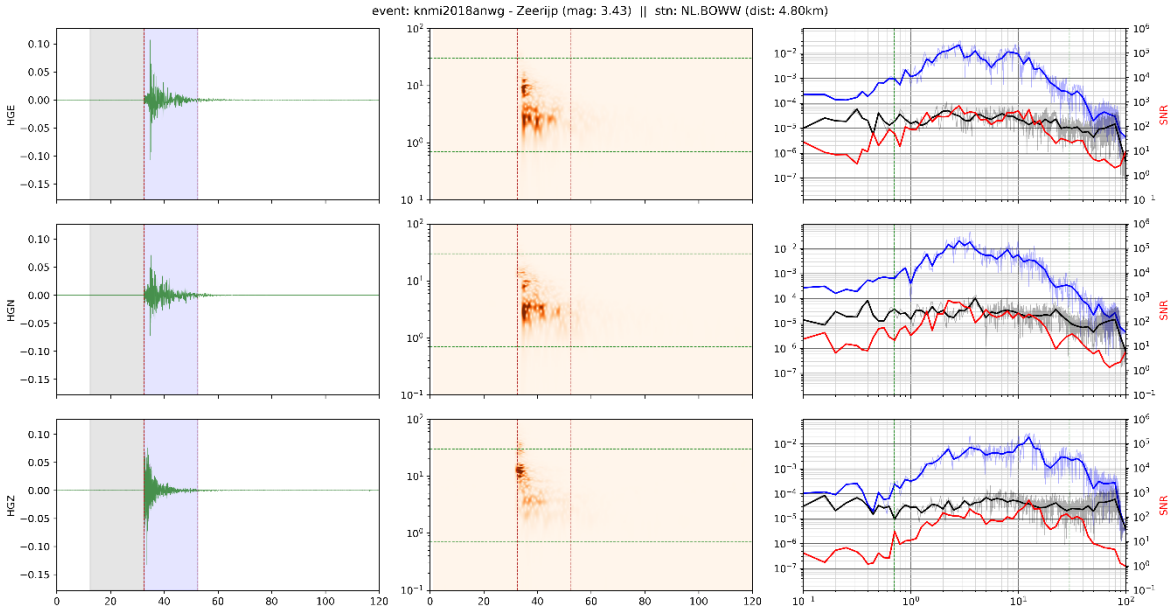

Figure III.2 BOWW - Hellum 2015 (12 km)

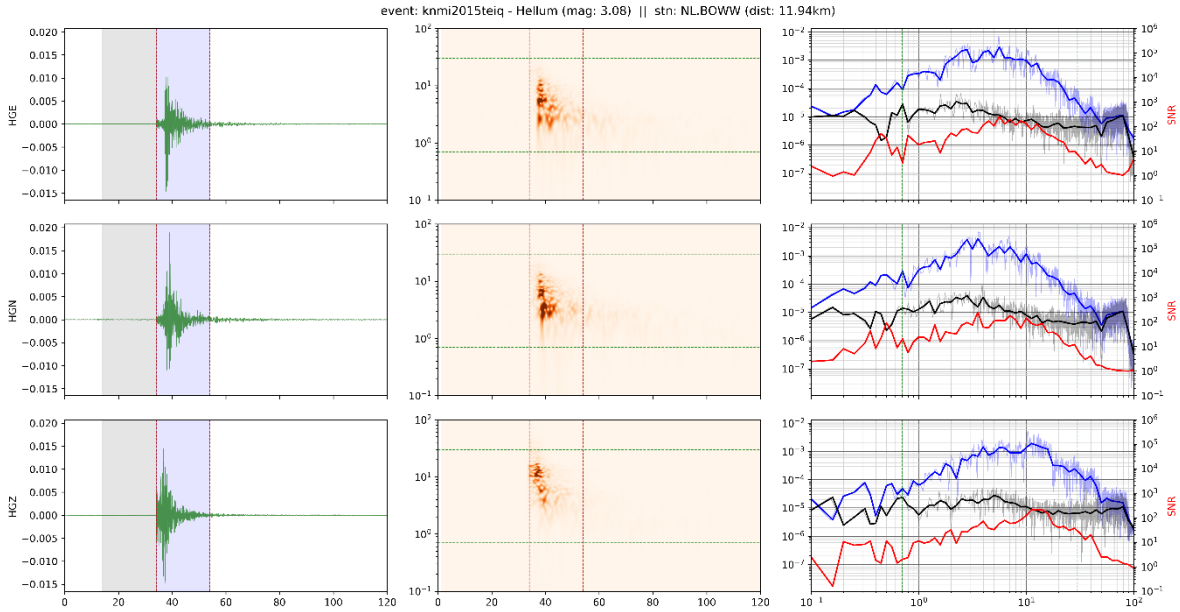

Figure III.3 BOWW - Gamerwolde 2014 (14 km)

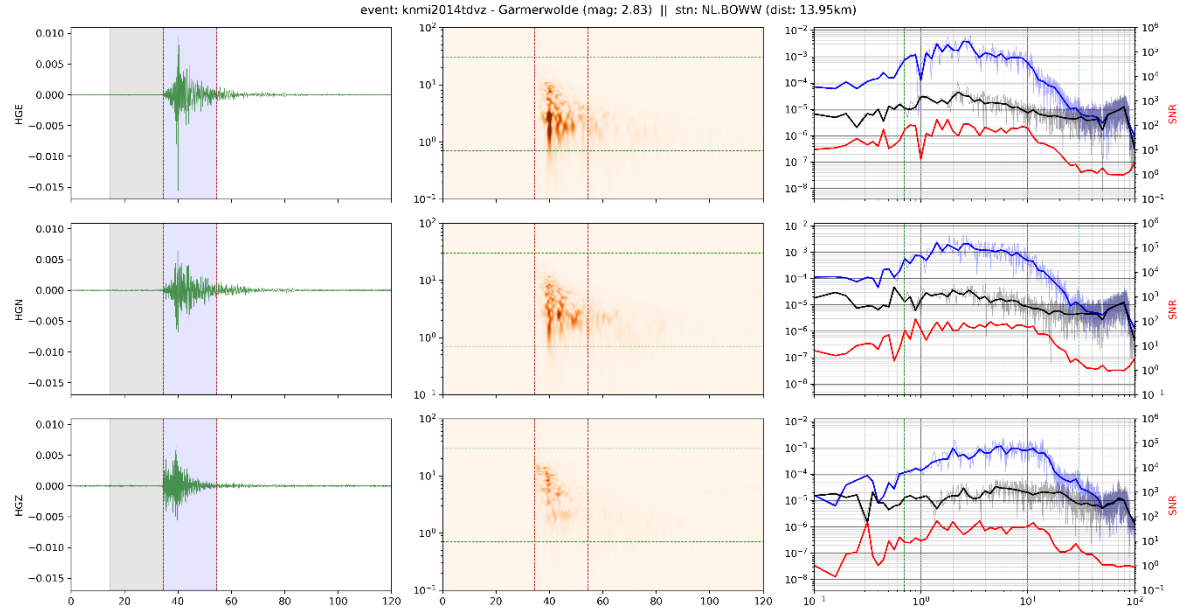

Figure III.4 BOWW - Zandeweer 2014 (10km)

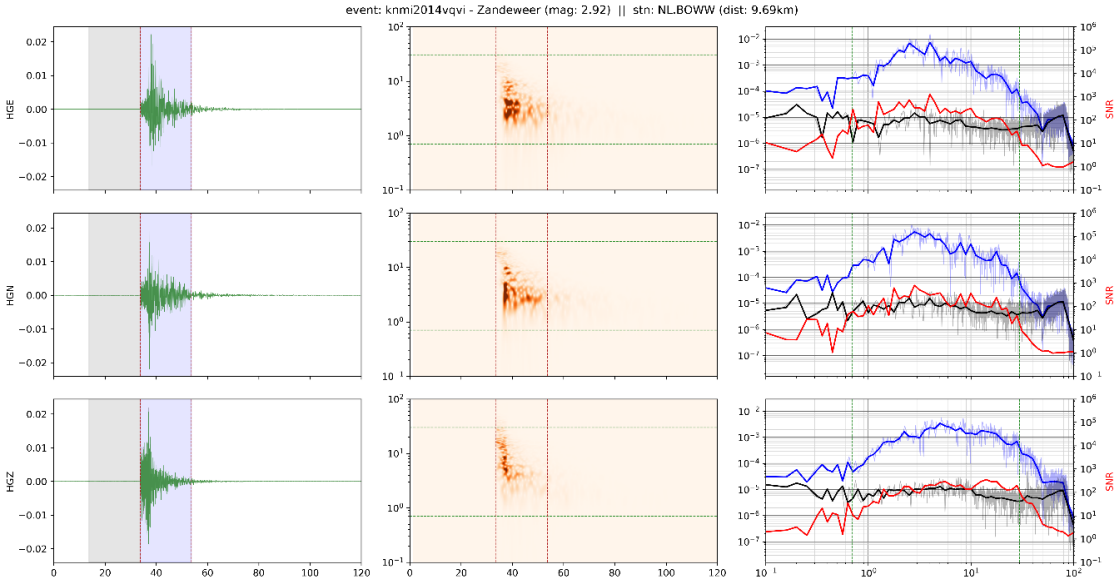

Figure III.5 BAPP - Garmerwolde 2014 (14km)

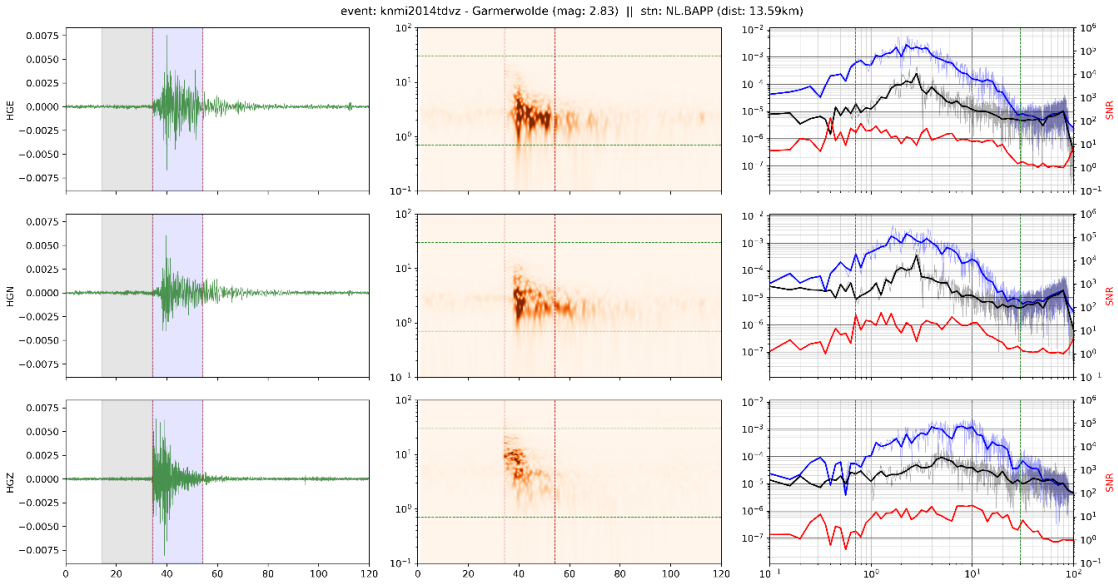

Figure III.6 BAPP - Zandeweer 2014 (12.5km)

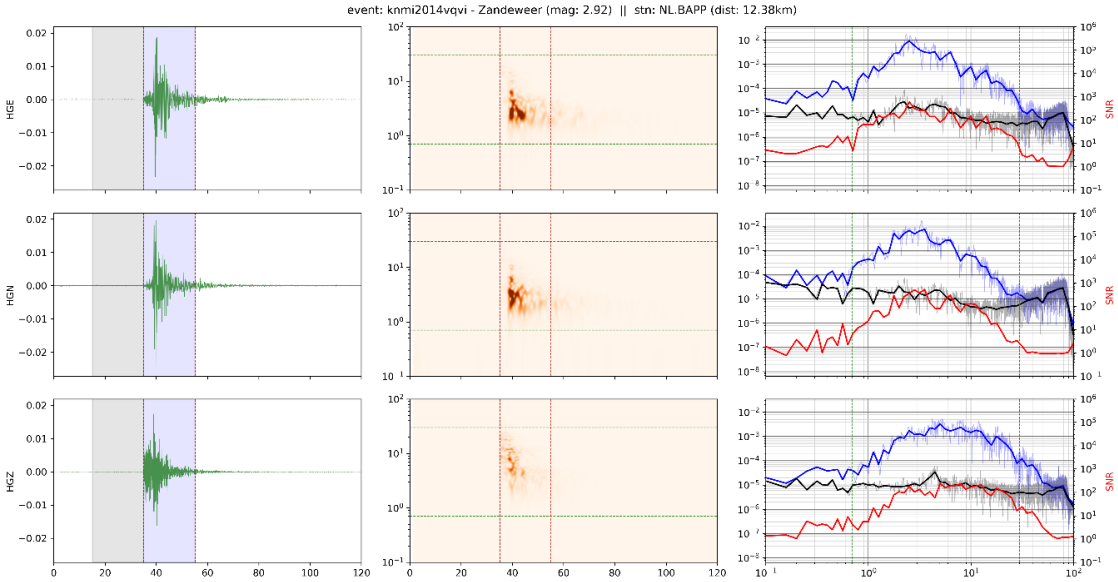

Figure III.7 BAPP - Zeerijp 2018 (8km)

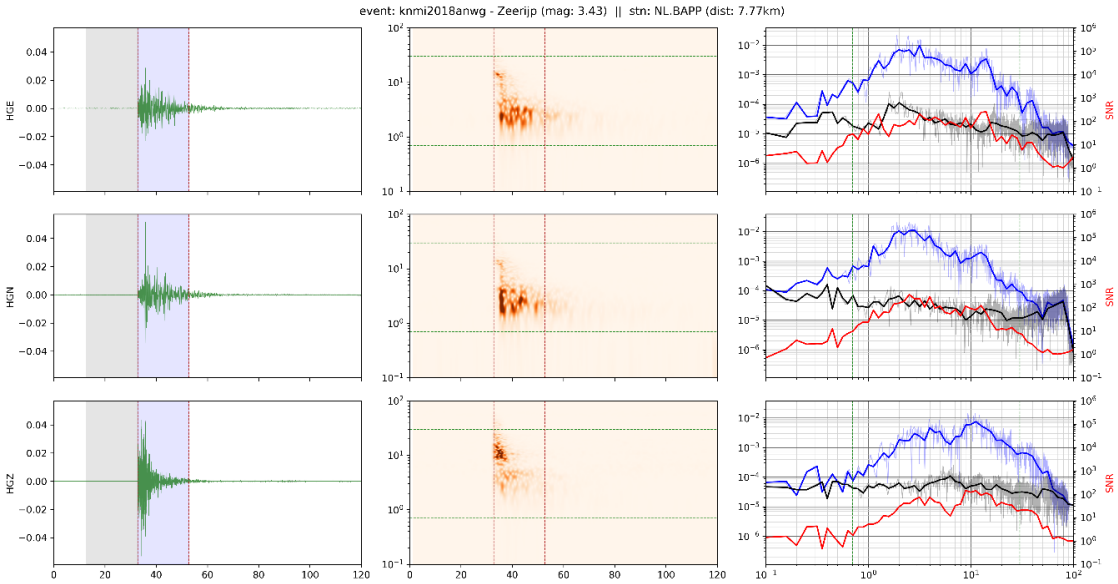

Figure III.8 BAPP - Hellum 2015 (9km

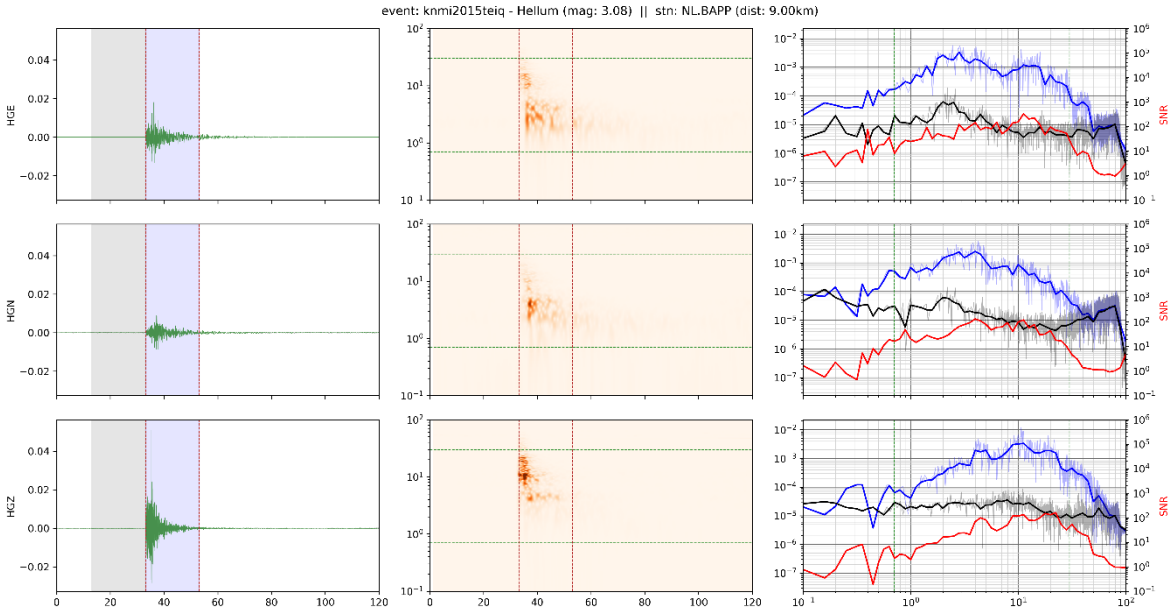

Figure III.9 BSTD - Zeerijp 2018 (7km)

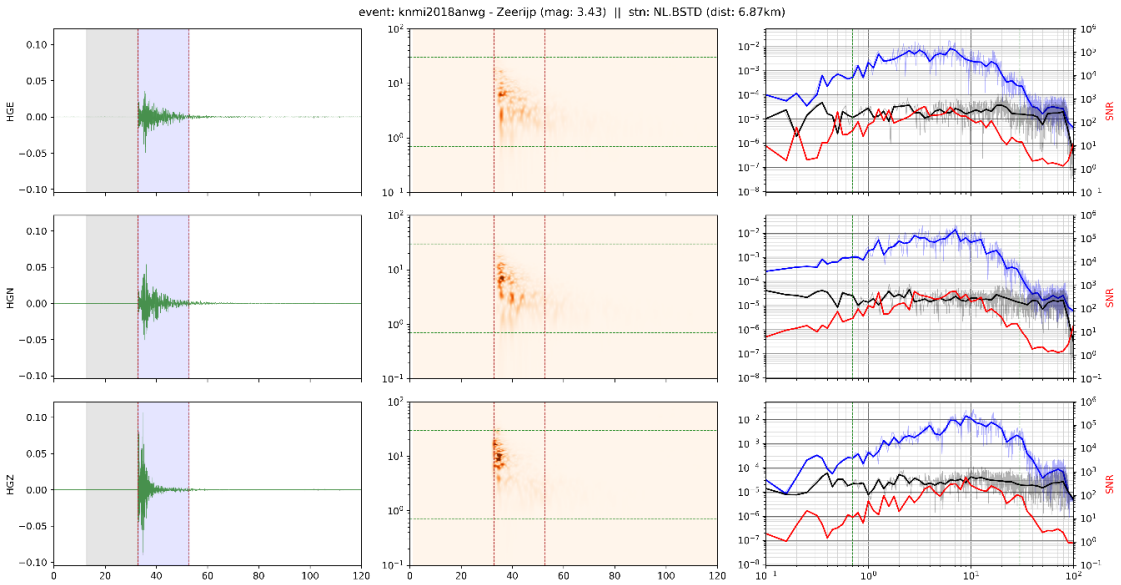

Figure III.10 BSTD - Hellum 2015 (13km)

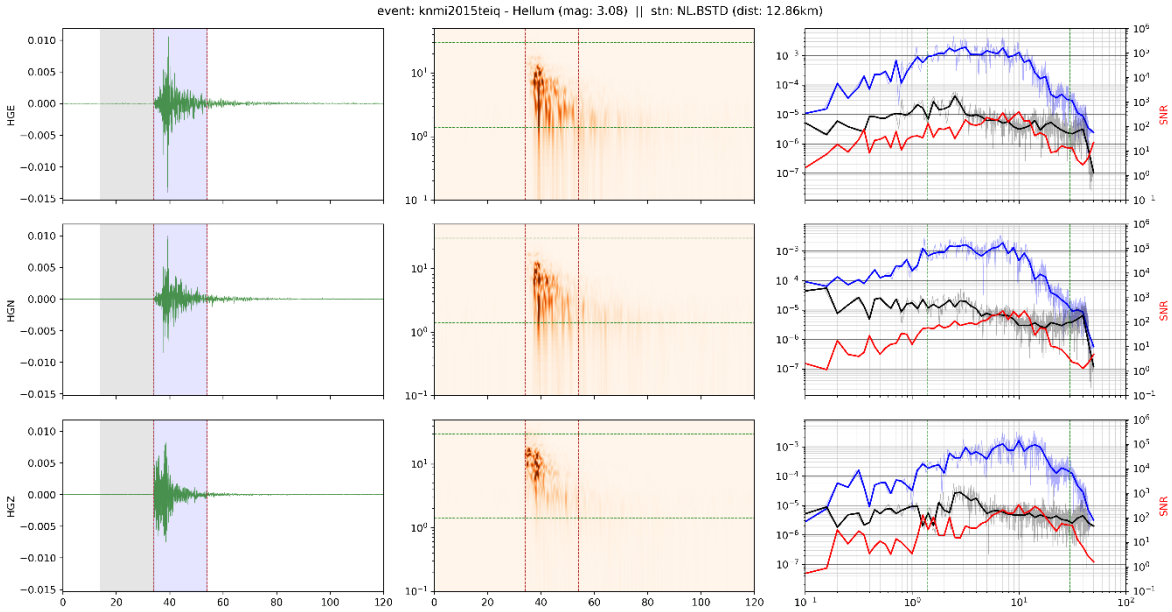

Figure III.11 BSTD - Garmerwolde 2014 (6.5km)

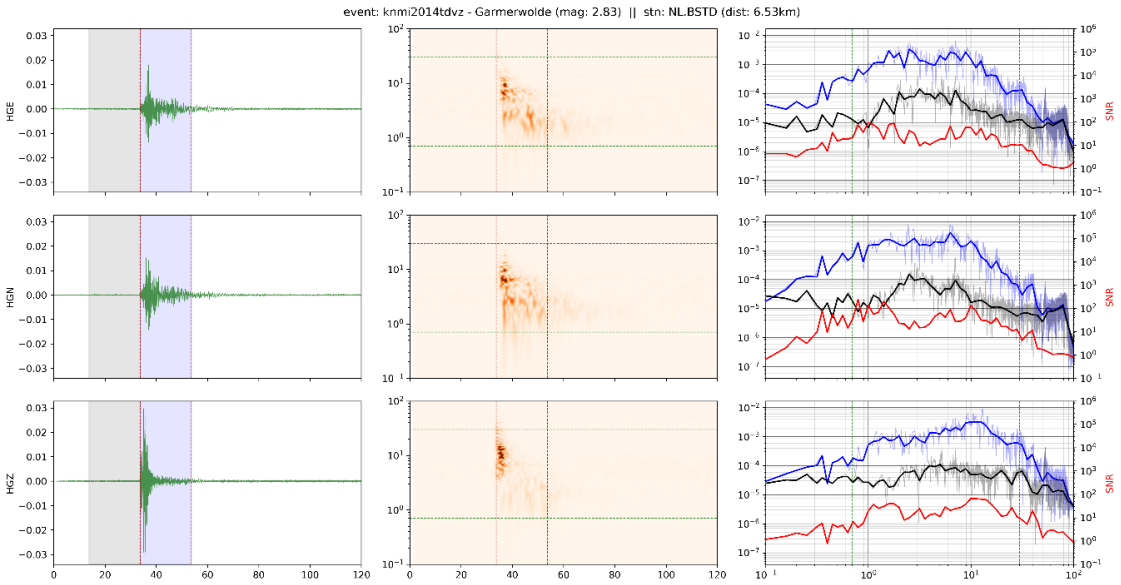

Figure III.12 BSTD - Zandeweer 2014 (7km)

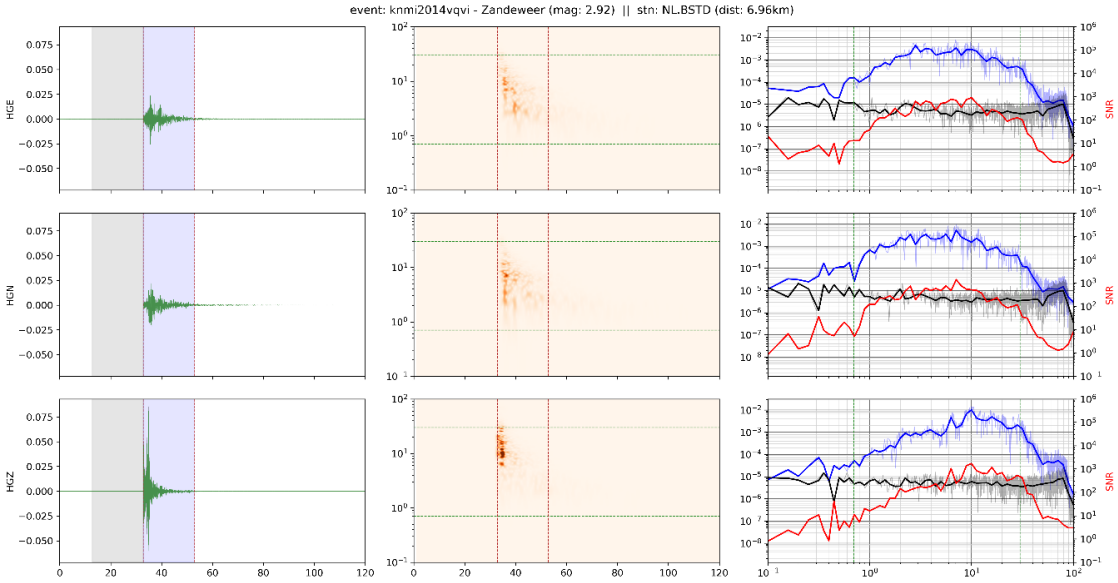

Figure III.13 BFB2 - Garmerwolde 2014 (11km)

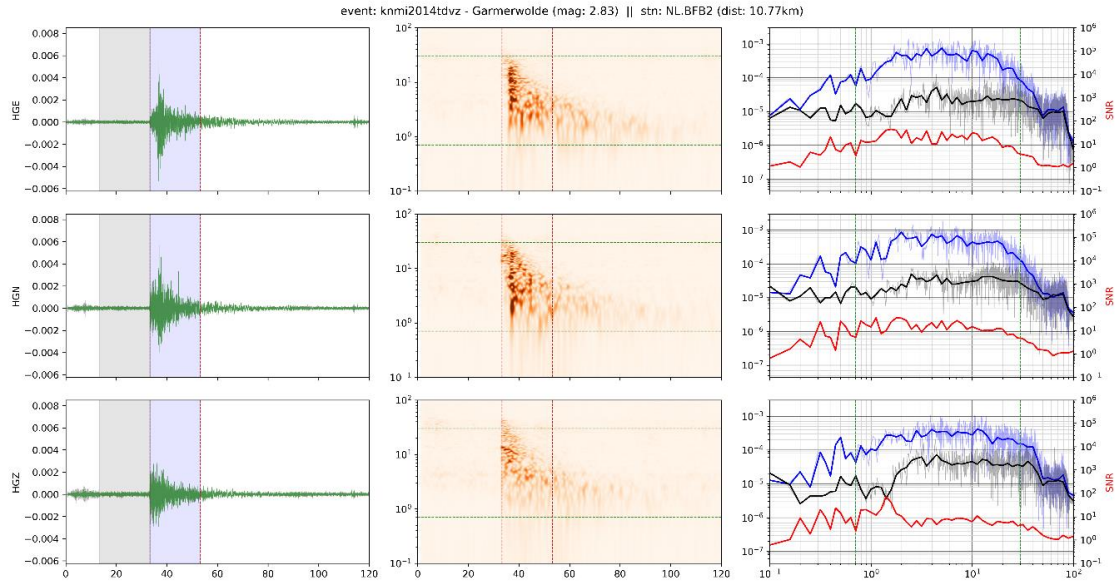

Figure III.14 BFB2 - Zandeweer 2014 (22km)

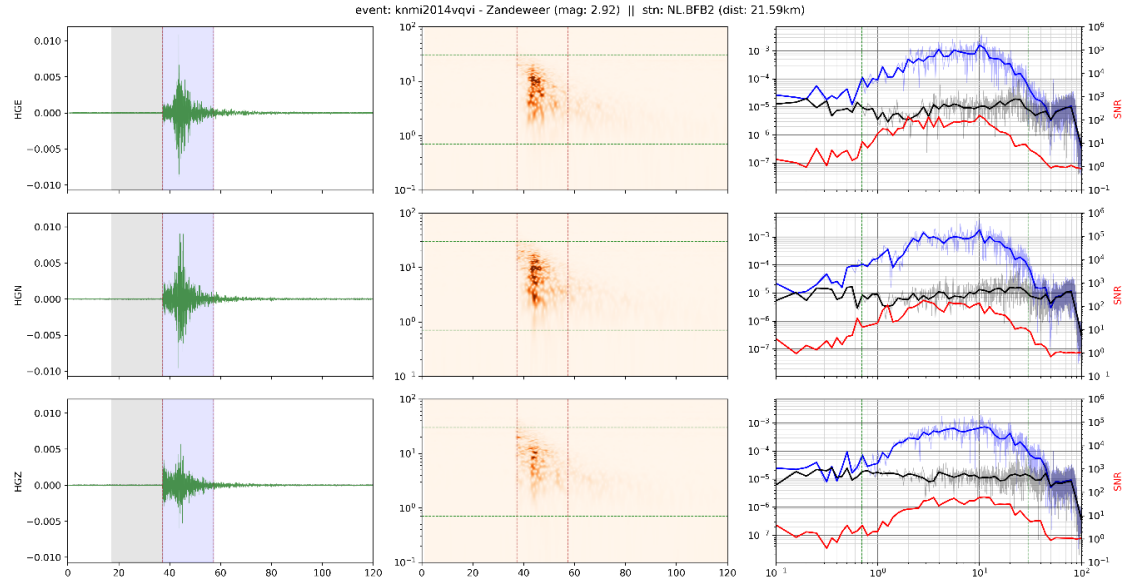

Figure III.15 BFB2 - Zeerijp 2018 (19.5km)

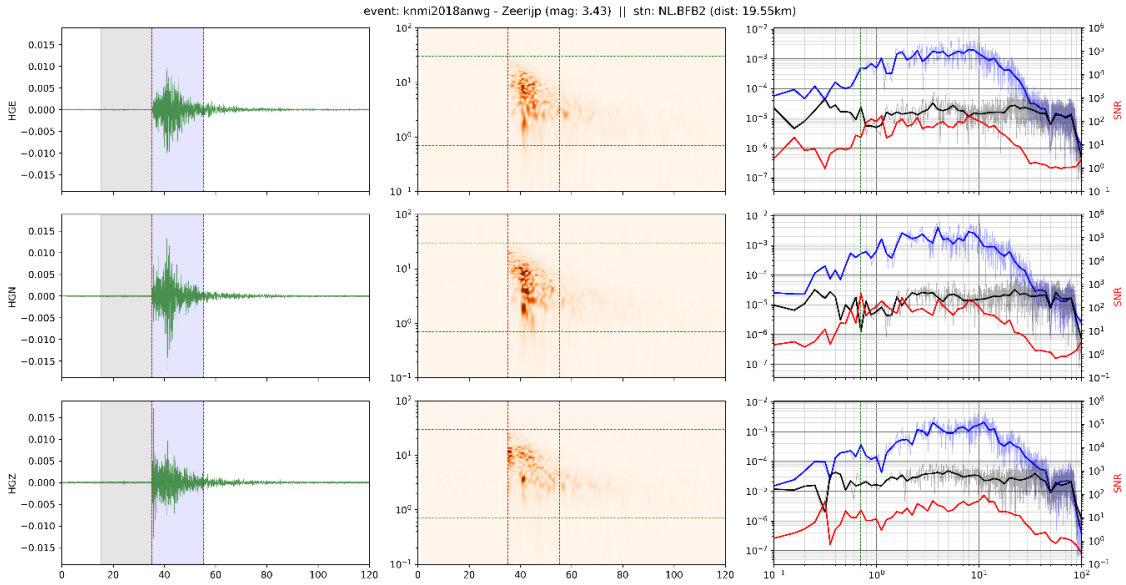

Figure III.16 BFB2 - Hellum 2015 (7km)